In presenting the dissertation as a partial fulfillment of the requirements for an advanced degree from the Georgia Institute of Technology, I agree that the Library of the Institute shall make it available for inspection and circulation in accordance with its regulations governing materials of this type. I agree that permission to copy from, or to publish from, this dissertation may be granted by the professor under whose direction it was written, or, in his absence, by the Dean of the Graduate Division when such copying or publication is solely for scholarly purposes and does not involve potential financial gain. It is understood that any copying from, or publication of, this dissertation which involves potential financial gain will not be allowed without written permission.

7/25/68

AN INVESTIGATION OF ELECTROCHEMICAL FACTORS INVOLVED IN THE STRESS CORROSION CRACKING OF TITANIUM ALLOYS IN SALT SOLUTIONS

A THESIS

Presented to

The Faculty of the Graduate Division

by

Fu-Shiong Lin

In Partial Fulfillment

of the Requirements for the Degree

Master of Science in Metallurgy

Georgia Institute of Technology

June, 1971

AN INVESTIGATION OF ELECTROCHEMICAL FACTORS INVOLVED IN THE STRESS CORROSION CRACKING OF TITANIUM ALLOYS IN SALT SOLUTIONS

Approved:

Chairman

Date approved by Chairman: 6-2-71

ACKNOWLEDGMENTS

I wish to express my sincere appreciation and gratitude to Dr. R. F. Hochman, my thesis advisor, for his guidance, encouragement and patience during this study. I also wish to thank Dr. E. A. Starke, Jr. and Dr. Helen Grenga for their review of this work.

I am grateful to the Advanced Research Project Agency, ARPA order 878, for the support which made this investigation possible.

TABLE OF CONTENTS

TABLE OF CONTENTS (Continued)

LIST OF TABLES

LIST OF FIGURES

LIST OF FIGURES (Continued)

LIST OF FIGURES (Continued)

LIST OF FIGURES (Concluded)

SUMMARY

The material used in this study was commercial Ti:8-1-1 alloy. Corrosion studies were made in salt solutions of different pH values. The potential, current and polarization curves of unstressed and stressed specimens under tension and bending were measured with "Beckman Electroscan 30" potentiostat.

The current density between a fresh surface and a normal air exposed surface of Ti:8-1-1 alloy is about 2 mA/cm^2. The electrode potential of fresh surface specimens is dependent on the pH value of the solution, i.e. -0.88 and -1.02 volt (SCE) in NaCl solutions with pH = 3.5 and 11.5 respectively.

The results indicate that crack initiation may involve preferential dissolution at the head of dislocation pile-ups. In addition, anodic dissolution at the crack tip is possible and may play some part in crack propagation.

A region in the potential and the current versus time curves was directly related to the crack propagation and indicated that crack propagation was continuous.

CHAPTER I

INTRODUCTION

Stress corrosion cracking can be defined as a cracking process that is caused by the simultaneous application of a corrodent and sustained tensile stress (1). Generally titanium base alloys are resistant to stress corrosion cracking. These alloys normally have a good protective film, however, it can be ruptured by applied tensile stresses. Electrochemical cells will develop between the bare surface and the film-covered surface that will prevent film repair and enhance anodic dissolution (2, 3). Unlig (4), Uhlig and Sava (5), and Coleman and coworkers (6) have suggested that the adsorption of atoms or ions in the stress-corrosion medium on the metal at the tip of the crack may be a factor in the stress corrosion cracking of metals because chemisorption decreases the surface energy at the crack tip. Scully (7) and others have suggested that hydrogen plays an important role in the stress corrosion cracking. The hydrogen ions in the corroding medium will be discharged and then diffuse into the metal when the surface film is ruptured. It has also been suggested that the hydride phase may be precipitated within the plastic zone of the crack tip, embrittling it.

There is much disagreement in the literature concerning the possible role of hydrogen, surface energy and/or anodic dissolution in the stress corrosion cracking process. The present study concerns itself with the electrochemical aspects and the role of anodic dissolution

in the stress corrosion cracking process of titanium alloys.

Titanium-Hydrogen System

A phase diagram of the Ti-H system, based on the data by Livanov (8), is shown in Figure 1. A diagram indicating the solubility of hydrogen in α-titanium from this data is shown in Figure 2. Figure 3 shows how the aluminum content in titanium alloys affects the solubility of hydrogen.

The phase diagram shows that hydrogen stabilizes the β-phase and narrows the α-phase region. The solubility of hydrogen in α-titanium decreases sharply with decreasing temperature. Titanium hydride precipitates have been confirmed by autoradiography, with the aid of tritium, the radioactive isotope of hydrogen (9). The hydride ($TiH_{1.7-2.0}$) has a face-centered cubic lattice (8) with the hydrogen atoms occupying the tetrahedral interstitial positions (10). It appears that the octahedral vacancies are too large for the hydrogen atoms and in the larger space the hydrogen atoms may have increased vibration energy which results in instability (8). Jaffee (11) found that titanium hydride with higher hydrogen contents larger than 66 atomic percent has a tetragonal and not a cubic lattice. This has been explained as distortion by hydrogen atoms in the interstitial positions with the result of a gradual transition from a cubic structure at low hydrogen content to a tetragonal structure at higher hydrogen compositions.

The hydride precipitates are usually formed along the slip planes (12), predominantly along $\{10\bar{1}0\}$ and $\{10\bar{1}1\}$. The orientation relationships between the α-titanium and hydride are:

$(10\bar{1}0)_{\alpha\text{-Ti}} || (101)_{\gamma}$, $[12\bar{1}0]_{\alpha\text{-Ti}} || [011]_{\gamma}$; $(10\bar{1}1)_{\alpha\text{-Ti}} || (101)_{\gamma}$, $[12\bar{1}0]_{\alpha\text{-Ti}} || [100]_{\gamma}$, where γ is the hydride phase.

The diffusion of hydrogen in α and β-titanium has been investigated by Papazoglon (13) and Wallewski (14). Their results showed that the diffusion coefficient of hydrogen in α-titanium is larger than that in β-titanium according to the following relations:

$$D_{\beta} = 1.95 \times 10^{-3} \exp\left(\frac{-6,640 \pm 500}{RT}\right) \text{ cm}^2/\text{sec} \qquad (1)$$

$$D_{\alpha} = 1.8 \times 10^{-2} \exp\left(\frac{-12,380 \pm 680}{RT}\right) \text{ cm}^2/\text{sec} \qquad (2)$$

where D is diffusion coefficient, R is gas constant and T is temperature in Kelvin scale.

Hydrogen Embrittlement of Titanium Alloys

As mentioned in the introduction hydrogen is a very harmful impurity in titanium alloys and may cause brittleness and cracking if present as titanium hydride precipitates (7, 8, 15). The solubility of hydrogen in titanium decreases sharply with decreasing temperature being only 40 ppm or less at room temperature (15). The majority of the hydride platelets formed at low hydrogen concentrations have a specific habit plane and most of the platelets are precipitated within the grains rather than at grain boundaries (16). The hydride phase in hydrogen-containing α/β alloys occurs in highly localized areas. Williams (15) has shown that hydrides form preferentially at the α/β interface and highly localized hydride precipitation is occasionally observed in the stressed regions and on the planes perpendicular to

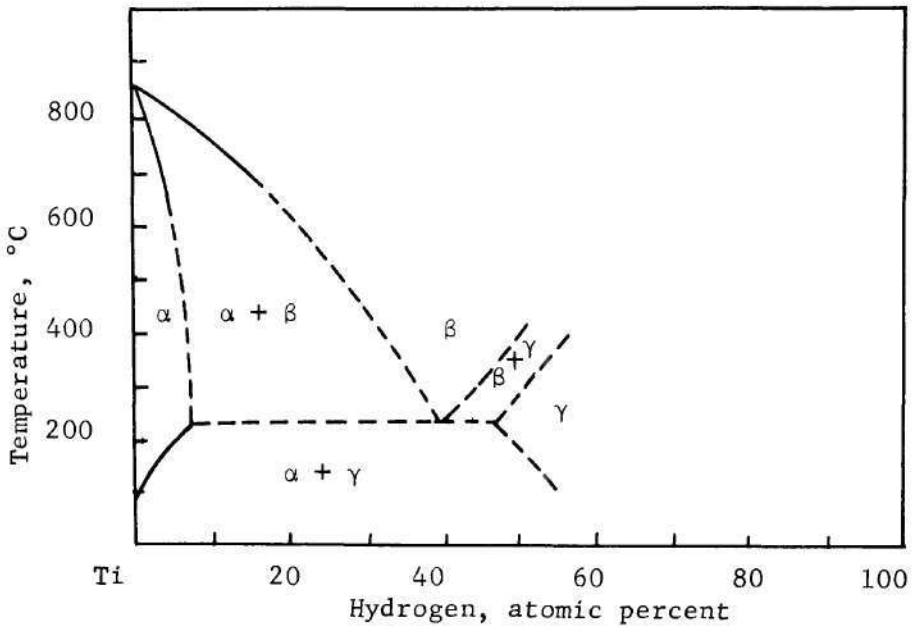

Figure 1. Phase Diagram of the Ti-H System.

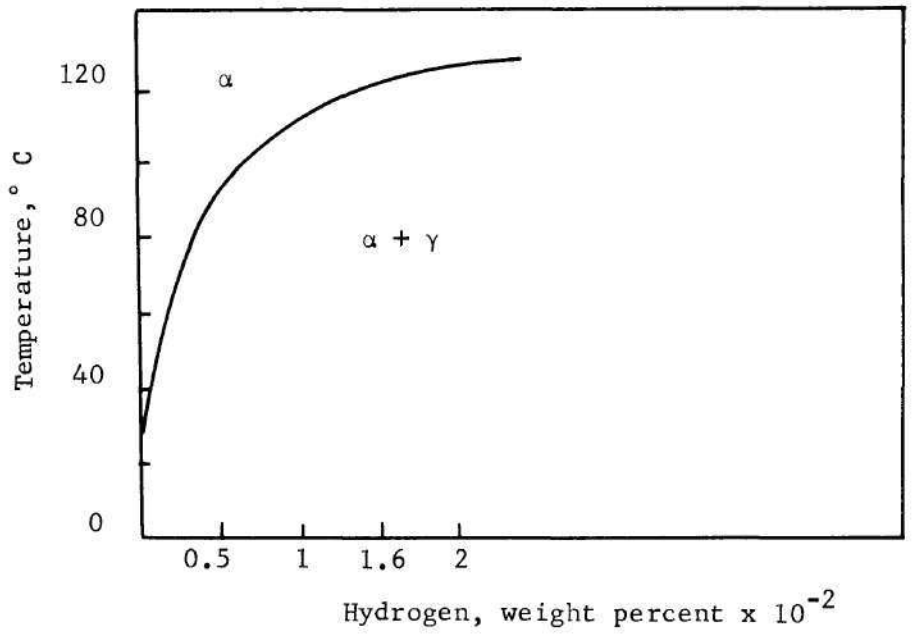

Figure 2. Solubility of Hydrogen in α-titanium

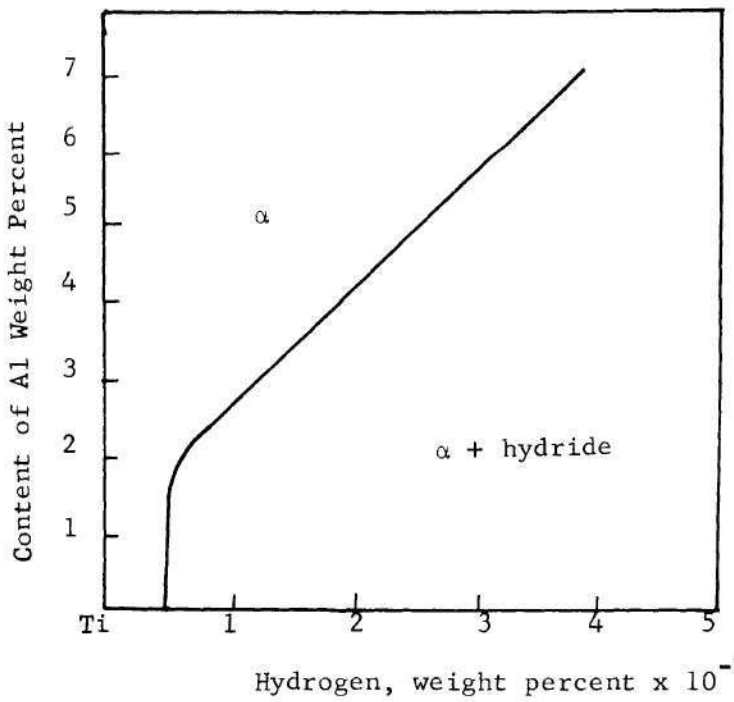

Figure 3. Isothermal Cross Section of the Phase Diagram of the Ti-Al-H System at 20°C.

the principal applied tensile stress (16, 17). If the stress is high enough, cracking may occur along the hydride phase.

It is probable that the presence of the hydride acts in two ways; through its ability to act as a stress-raiser and its inherent brittleness which results in the introduction of microcracks (15). Mauney and Starke (18) have suggested that since the Ti-hydrides form on the $\{10\bar{1}0\}$ and $\{10\bar{1}1\}$ planes, slip is impeded on these planes. This results in dislocation pile-ups of the $<11\bar{2}3>$ type on $\{11\bar{2}2\}$ planes if six percent or greater aluminum impedes slip on the basal plane. The most likely cleavage plane predicted by this mechanism was a plane that made an angle of 70.5 degrees with the pile-up's slip planes, i.e. $\{10\bar{1}7\}$ or $\{10\bar{1}8\}$ planes.

The great sensitivity of titanium alloys to hydrogen embrittlement occurs in the presence of notches and at low temperatures (8). The hydrogen embrittlement of $(\alpha + \beta)$ alloys is observed only at very low deformation rates (8). The β-phase does not become brittle even at high hydrogen concentrations and acts as a crack arrestor in $(\alpha + \beta)$ alloys (20, 22, 23). However, for the β-phase to act as crack arrestor in an α-matrix, it must be lamellar and randomly distributed.

The previous two paragraphs indicate that the function of excess hydrogen in titanium is probably the formation of hydride precipitates. Hydride precipitates are observed when hydrogen is adsorbed and absorbed by titanium alloys in acidic pickling baths (24), in chemical polishing and electropolishing solutions (25), in hydrogen gas baths (15), etc. However, no hydride precipitates have ever been directly identified in titanium alloys after stress corrosion tests in NaCl solutions.

An Electrochemical Mechanism of Stress Corrosion Cracking

Logan (2), Dix (26), Pickering (27), and others postulated that alloys which undergo stress corrosion cracking in a specific environment have protective films. When stressed, the film ruptures locally, exposing fresh surface which is highly anodic. Stress corrosion cracking is therefore suggested to be electrochemical dissolution. They also suggested that the anodic dissolution is concentrated at the crack tip because the metal at that point is continuously yielding. The yielding prevents the formation of the passive film, and anodic dissolution is continuous. Hines (57) indicated that the yielding also reduces the activation polarization which favors anodic dissolution at the crack tip. Uhlig (58) suggested that the anodic dissolution and the decrease of the surface energy at the crack tip due to adsorbed species is also important in the stress corrosion cracking process. The mechanochemical model, proposed by Hoar (59), is based on mechanical tearing of the metal and anodic dissolution, i.e. that deforming film-free metal (at the crack tip) is anodic relative to non-deforming material (at the crack walls). There is abundant evidence that electrochemical processes play a major part in stress corrosion cracking of metals in aqueous solutions.

Deformation Modes

There are three possible slip planes in α-titanium (31, 33), (0001), $\{10\bar{1}0\}$ and $\{10\bar{1}1\}$, all of which slip in $\langle 11\bar{2}0\rangle$ directions. The twinning planes are $\{1\bar{1}02\}$, and $\{11\bar{2}k\}$ where k is 1, 2, 3 and 4.

The detection of slip with a non-basal slip vector, probably of

the type $\frac{1}{3}\{11\bar{2}3\}$, has been made in both Ti and Ti-Al alloys (34), and has been observed to decrease with increasing aluminum content. The dislocations often appear to be paired, which may be a result of $\frac{1}{3}<11\bar{2}3>$ dissociation to <0001> and $\frac{1}{3}<11\bar{2}0>$ partial dislocations (25). Pickering (27) suggested that the presence of an ordered structure caused dislocation pile-ups and pairing. Most of the dislocations he observed were in pairs with a screw orientation. In the Ti-Al alloys, it has been found that $\{10\bar{1}0\}$ slip planes tend to predominate at low strain, but at higher strain slip on $\{10\bar{1}1\}$ and to a lesser extent on (0001) in $\frac{1}{3}$ $<11\bar{2}0>$ direction predominates (25, 26, 35). Interstitial atoms in the octahedral sites increases the probability of $\{10\bar{1}0\}$ slip (35, 36). Alloying with aluminum appears to cause inhibition of twinning, leaving slip the predominant form of deformation (35).

Aluminum Content and the Susceptibility to Stress Corrosion Cracking of Ti-Alloys

The Ti:8-1-1 alloy has been shown to be one of the most susceptible of all the titanium alloys to stress corrosion cracking. This is believed due to the formation of ordered Ti_3Al precipitates. The precipitates of Ti_3Al in Ti-Al alloys with aluminum contents above six percent by weight were confirmed by Crossley (41) and Blackburn (42). The ordered precipitates were found to cause a rearrangement of the dislocation distribution from cellular to co-planar arrays and to inhibit deformation by cross slip (39). Thus aluminum addition restricts the movement of dislocations in the $\{10\bar{1}0\}$ planes (25), decreases the twinning probability (35) and inhibits deformation by cross slip. This

results in more dislocation pile-ups which has been postulated as increasing stress corrosion susceptibility.

CHAPTER II

EXPERIMENTAL PROCEDURE

Specimen Preparation

The Ti:8-1-1 alloy used in this study was prepared by Titanium Metals Corporation of America. The specimens were in the mill annealed condition, degreased with benzene and acetone dried. Several different surface conditions of the unstressed specimens were used, ranging from a rough polished surface to a one micron polished finish. Unless otherwise stated, the specimens were in a machined surface finish. A dead weight tensile machine with a 1:20 arm ratio was used for the static tensile tests and the Standard Cantilever-Beam Machine with a 36-inch moment arm was used for the bending tests.

Polarization Curve Measurement

Stress corrosion cracking can be controlled by cathodic and anodic polarization. The former controls the discharge of hydrogen ions, which may then diffuse into the metal. The latter controls the anodic dissolution of titanium and the formation of compounds which may assist stress corrosion cracking. The anodic polarization of titanium and its alloys has been investigated in sulfuric acid (44, 45) and hydrochloric acid (46) at different concentrations, temperatures and alloy compositions. However, there is little or no data about anodic and cathodic polarization in sodium chloride solutions. The polarization test cell was basically the same as that described earlier by

Myers (47). The anodic and cathodic polarization of the unstressed specimens was measured for different surface conditions and pH values. The anodic polarization curves of unnotched and notched specimens under tensile and bending stresses were also measured.

The polarization curves were made using a "Beckman Electroscan 30" potentiostat with a saturated calomel electrode as a reference electrode and a platinum electrode as an auxiliary electrode. All experiments were performed in a 3.5 percent NaCl solution. A specimen shown in Figure 4 as another reference electrode is used only for a experiment to detect the surface effects. The specimen design for the unstressed tests is shown in Figure 5, the tensile specimens in Figures 6 and 7, and the bend test samples in Figures 8 and 9. All specimens were coated with Silastic RTV 70 so that only 1 cm^2 area was exposed.

Quantitative Determination of Repassivation Power in Aqueous Solution

Scully (51) suggested that the repassivation of Ti-alloys was delayed by the chloride ions at the emergent slip steps so that the hydrogen ions discharged at this point diffuse into the metal. This experiment was designed to determine the repassivation power of Ti:8-1-1 alloy in the various solutions. The specimen (Figure 5) is scratched by a sharpened, non-conductive glass bar and then the electrode potential change versus a saturated calomel electrode is measured. Referring to the diagram shown in Figure 10, the repassivation power (R.P.) is determined by the following formula:

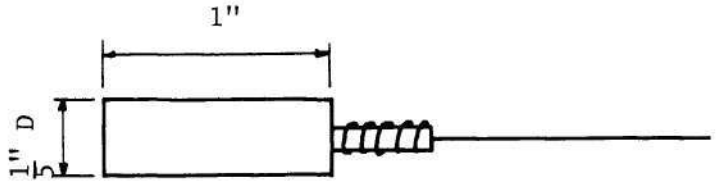

Figure 4. A Specimen as a Reference Electrode.

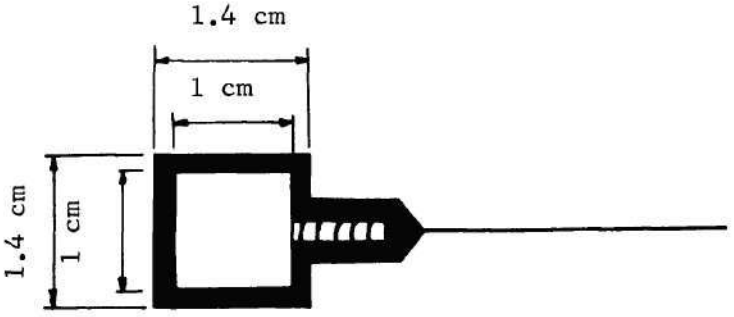

Figure 5. A Specimen Design for Unstressed Experiment. The Shadowed Area is Covered by Lucite with Copper as an Electrical Connection.

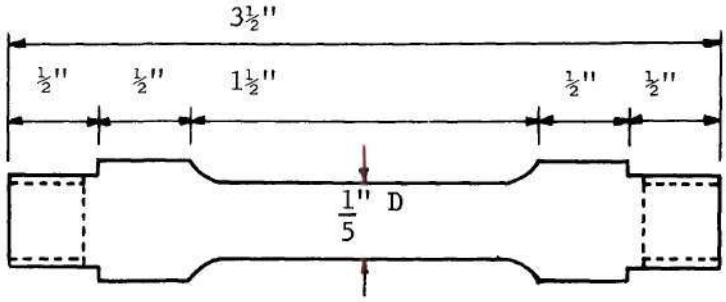

Figure 6. Specimen for Tension Tests.

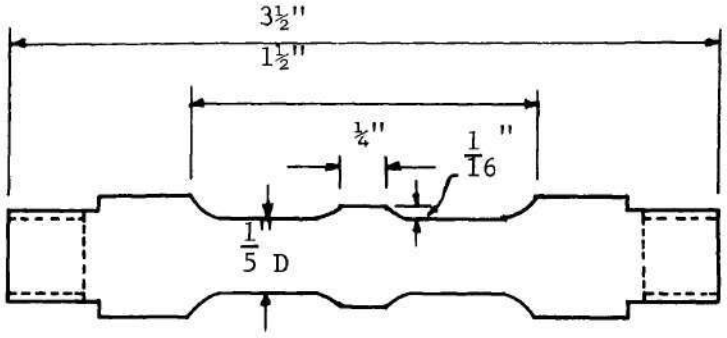

Figure 7. Special Specimen for Tension Tests to Detect Surface Effects.

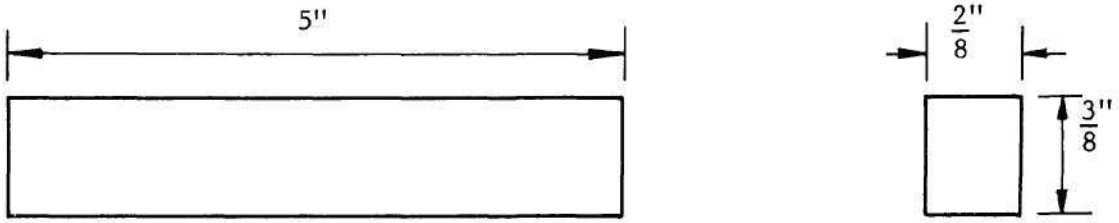

Figure 8. Specimen for Bending Tests.

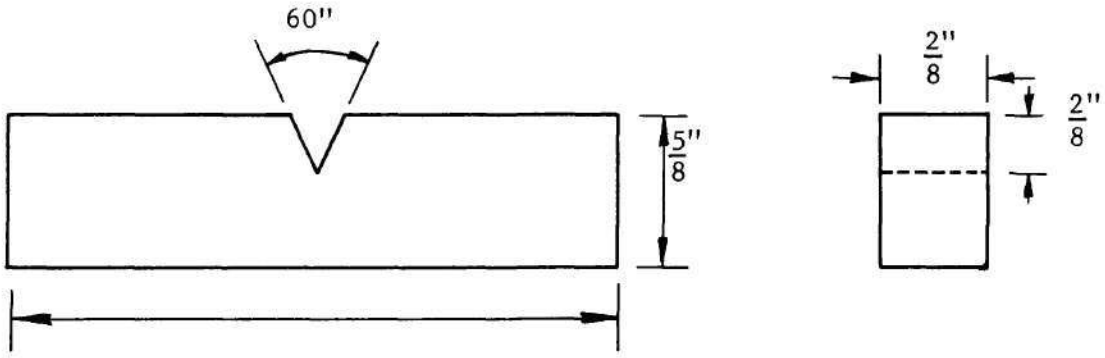

Figure 9. Notched Specimen for Bending Tests.

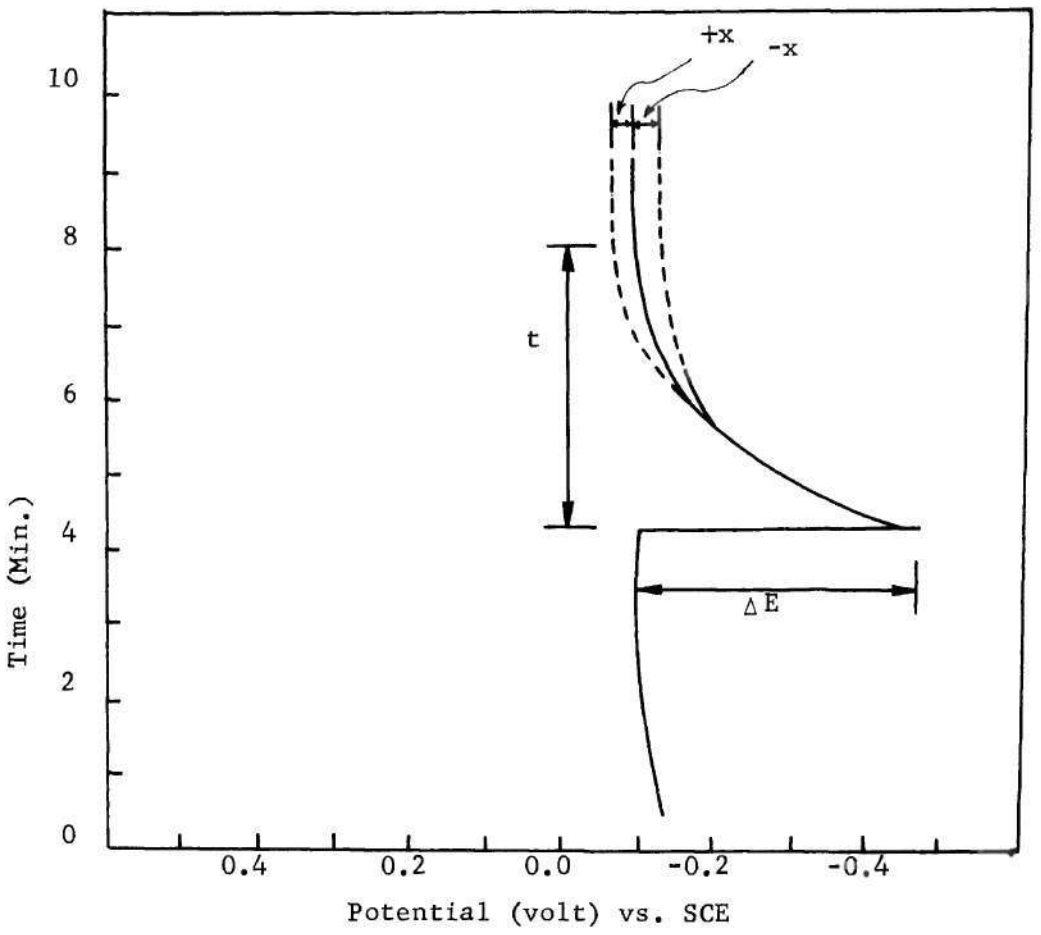

Figure 10. Typical diagram for the Calculation of the Repassivation Power for a Specimen Scratched by a Non-Conductive Material.

$$R.P. = \frac{\text{change of potential}}{\text{time for repassivation}}$$

$$= \frac{\Delta E \pm \text{deviation}}{\text{time}}$$

$$= \frac{\Delta E \pm X}{t} \text{ volt/min} \qquad (3)$$

where ΔE is the potential difference before and after scratching, X is the potential deviation dependent on solution and t is the time for the potential curve to reach a stable condition after scratching.

Surface Factor Investigation

Logan (2), Dix (26), Pickering (27) and others agree that the applied stress is helpful in rupturing the surface film, thereby exposing fresh metal at the tip of the crack and allowing the reactions to continue. The fresh surface is anodic with respect to the film-covered surface. Two specimens were used to study this phenomenon, one was polished through 3/0 emery paper and immediately immersed into the solution (fresh surface) acting as an anode. The other was polished and exposed to air for one week (film-covered surface) acting as a cathode. The current between the two electrodes was measured. The potential difference between these two specimens was also measured. Using several specimens polished and exposed to air for different times, the polarization characteristics for different surface conditions were obtained. The resulting current and potential curves are dependent on the length of time for passive film formation and growth.

Crack Initiation and Propagation Investigation

The progress of cracking was studied by removing unbroken specimens from the test machine at various times during the test. The surface of the specimen was examined for cracking and in some tests the specimen was then broken in air and the fracture surface examined by Scanning Electron Microscopy. Most specimens were removed after the potential had shifted to a more active value which was generally above the yield point.

To determine whether the crack propagation was continuous or discontinuous based on potential changes, the specimen was loaded above the yield point with only a small potential shift in the active direction. This condition was maintained until fracture occurred. The potential and current versus time curves were then examined for any discontinuity.

CHAPTER III

RESULTS

Current and Potential Measurement of the Stressed Specimens

Potentiostatic measurements were made on several unnotched samples in NaCl solutions under various loading conditions. The results of these studies are shown in Figures 11 and 12 as curves of potential and current versus tensile stress. It is noted that the potential shifts to a more active direction without repassivation when the stress exceeded 149,000 psi. Bending tests of unnotched specimens, on the other hand, were much less sensitive to applied stress, as can be seen from Figure 13. However, a sharp change of potential and current appeared during incremental loading of notched specimens during bending test (see Figure 14).

A faster chart speed was used to magnify the potential change within a short time interval around "A" in Figures 11, 12 and 13 as shown in Figures 15 and 16. The curves in these figures can be divided into four regions which can be correlated with the cracking process. This will be analyzed in the discussion.

The average rate of crack propagation was estimated to be about 0.042 cm/sec for smooth bend specimens. The rate was dependent on the dimensions of specimens and the level of stresses applied. The cracking rate was approximated by measuring the length of the crack and dividing it by the period of time of crack propagation.

Quantitative Determination of the Repassivation Power in Aqueous Solutions

The repassivation power of Ti:8-1-1 alloy in different solutions is listed in Table 1. These results imply that the delay of repassivation of Ti:8-1-1 alloy in $NaNO_3$ solutions is greater than that in NaCl solutions. However, Ti:8-1-1 alloy is not susceptible to stress corrosion cracking in $NaNO_3$ solutions (52).

Polarization Behavior

The discharge of hydrogen ions may be controlled by cathodic polarization, while the anodic polarization seems to control the anodic dissolution and the formation of the oxide. The reactions at both electrodes may be clarified by the behavior of anodic and cathodic polarization. The applied potential was repeated several times in a given range of the polarization curve; for example, from 0.6 to 1.6 volt (SCE) shown in Figure 20. During this test the surface of the specimen became a light yellow and turned darker with increasing potential. This may be due to the formation of titanium oxide which can occur in this range. Pitting was observed under the microscope (Figure 21) for potentials above 1.6 volt.

The cathodic polarization curve is shown in Figure 22. The small current measured during the potential change from 0.0 to -0.5 volt may be due to the residual current and a small amount of hydrogen ions being discharged at the surface. A lot of hydrogen ions will be discharged from -0.5 to -0.8 volt. No increase in current was observed in the -0.8 to -1.1 volt range. This may be due to the concentration polarization,

the activation polarization for the oxygen adsorption and for the formation of hydrogen molecules.

There is little or no data available in the literature about the reaction potential of titanium and chloride ions, but free energy data are available (48). The reaction potential can be calculated from the formula, $\Delta G = -nEF$, where G is the Gibbs free energy, E is the electrode potential, F is Faraday's constant and n is the metal valence. The free energy change of these reactions was calculated at 25°C considering ions at unit activity. This is a very approximate calculation but the general trends of these data, shown in Table 2 is useful in developing an understanding of the reaction. The electrode potential calculated from the free energy change is listed in Table 3. The results of this calculation indicated that the reactions between titanium, aluminum and chloride ions are spontaneous, i.e. the formation of titanium and aluminum chloride in NaCl solution during stress corrosion cracking is possible. The reaction does depend, however, on the surface condition of the metal and the pH value. The low pH value at the crack tip (53), which is about 1.7, favors chloride formation. These reactions may occur at the active site of the crack tip and may assist the cracking since $TiCl_4$ is liquid; $TiCl_3$ and $AlCl_3$ are soluble in water (49, 50).

pH Value, Surface Finish and Stress Corrosion Cracking

The stress corrosion cracking of titanium alloys can be correlated with the pH value and surface conditions. The relationships between them are shown in Figures 23 and 24 which indicate that the lower the pH value of the solution or the rougher the surface of specimen, the

lower the load needed for fracture.

The polarization behavior of Ti:8-1-1 alloy for different pH values of solution and surface conditions is shown in Figures 25 to 29. These curves indicate that the lower the pH value of the solution or the rougher the surface of specimens, the higher the anodic and the cathodic current densities, and the easier the discharge of hydrogen ions. Therefore, titanium alloys were more susceptible to stress corrosion cracking under these conditions. These Figures also indicate that the less exposure time in air, the higher the anodic current density is.

Effect of Scratching the Surface on Potential and Current Change

This experiment was conducted to determine the effect of discontinuities of the surface film on the measured potential in a NaCl solution. When the oxide film was broken by scratching, the potential and the current shifted sharply in the active direction but soon repassivated as shown in Figure 30. This figure also indicates that the pH value of the NaCl solution affects the electrode potential of the fresh surface (-0.88 and -1.02 volt (SCE) in NaCl solution with pH = 3.5 and 11.5 respectively). Figure 31 shows that the current between the film-covered surface and the fresh surface is about 2 mA/cm^2 (curve 1), and the potential difference between these two surfaces is about 1.0 volt.

Anodic Polarization Curves of the Stressed Specimens Prior to and After Crack Formation

The effects of stress on anodic polarization curves are shown

in Figure 32. The active region appears on these curves when the specimens were stressed above the yield point in NaCl solutions. The anodic polarization curves during cracking are shown in Figure 33. No passive region appears in these curves and the corrosion current increases continuously with increasing potential.

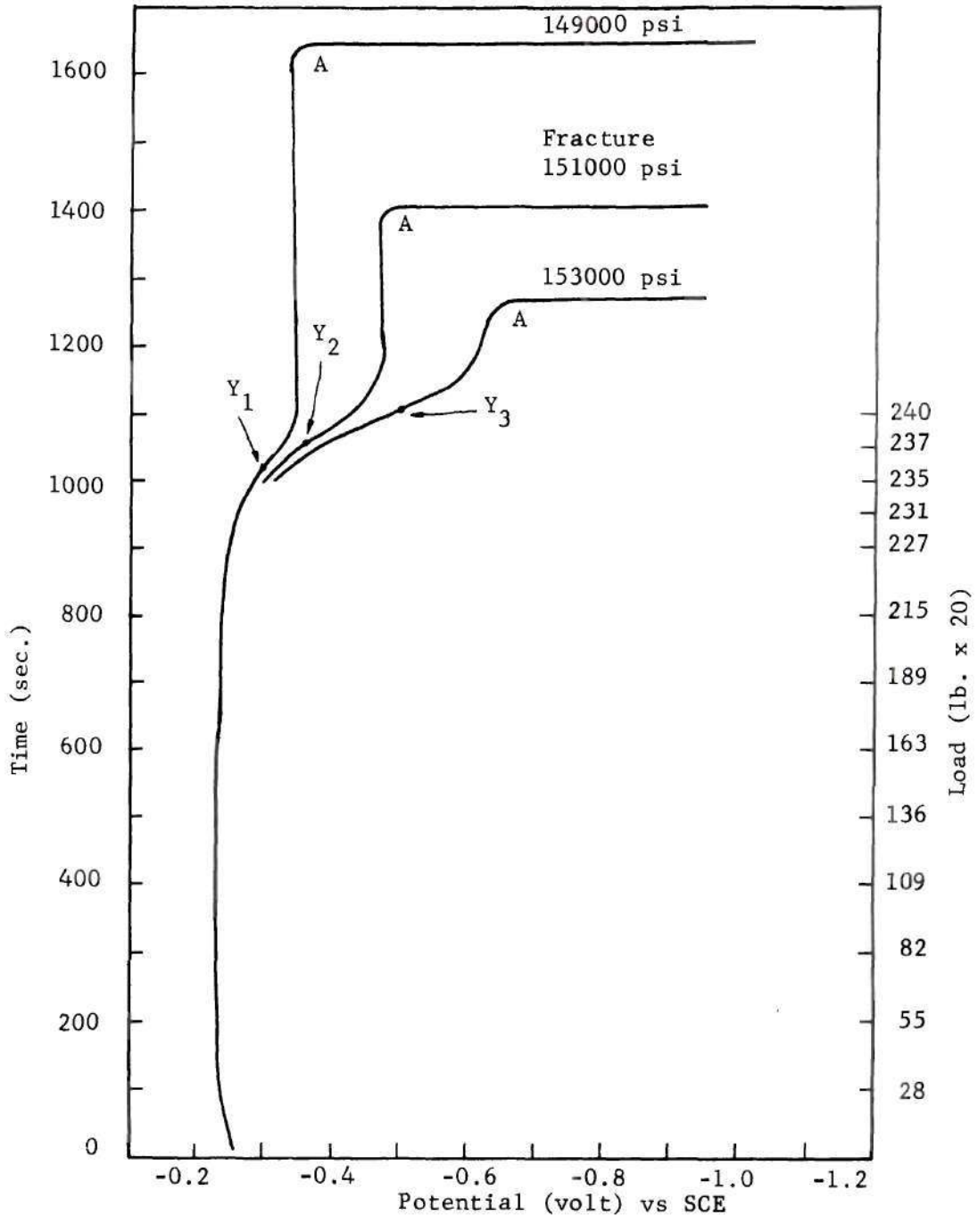

Figure 11. Potential vs Time Curves of the Specimens with Different Tensile Stresses in a NaCl Solution with pH = 3.5. Load eld Constant after Points Y_1, Y_2 and Y_3.

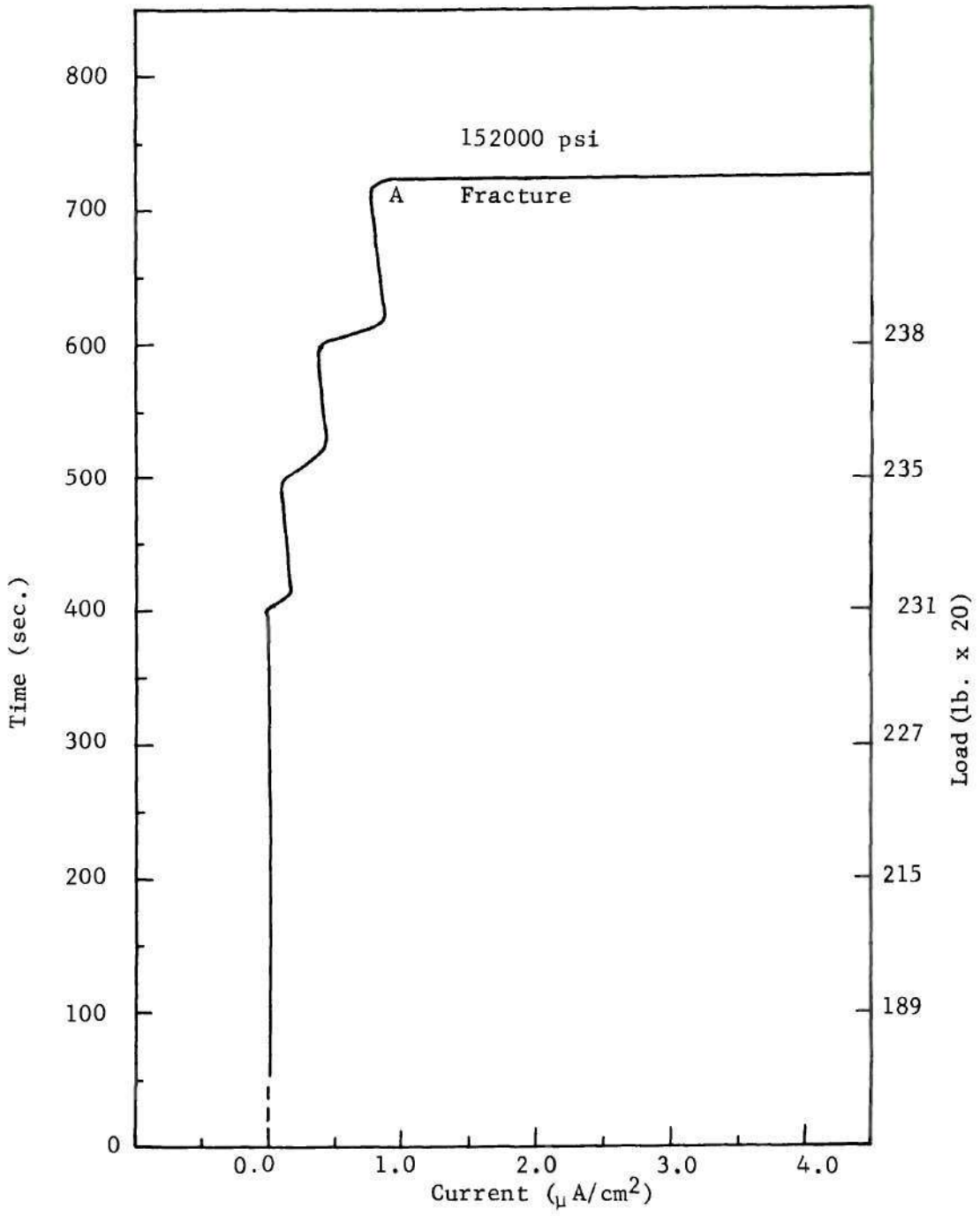

Figure 12. Current vs Time Curve of a Specimen under Tension in a NaCl Solution with pH = 3.5.

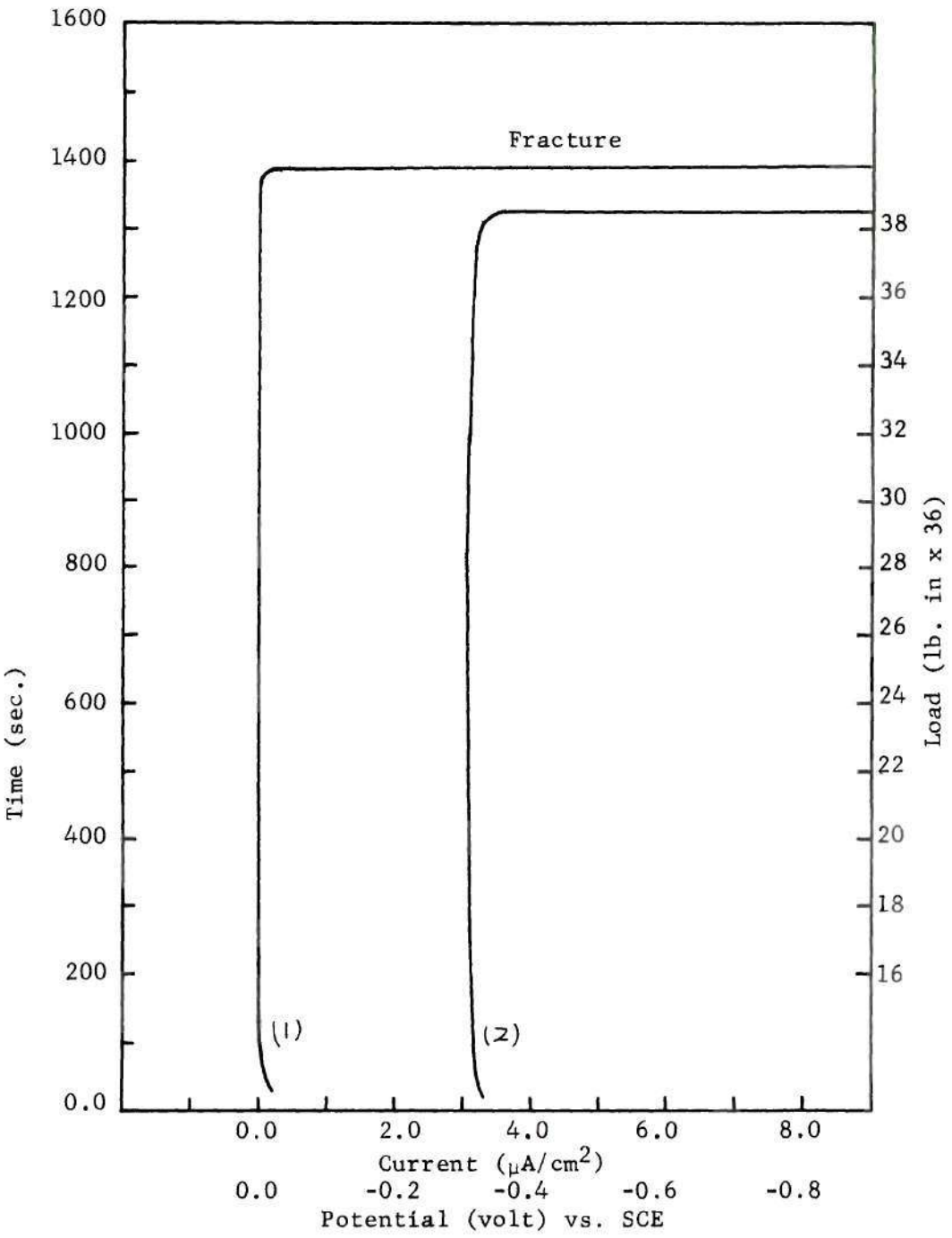

Figure 13. (1) Current vs Time and (2) Potential vs Time Curves of Specimens under Bending in a NaCl Solution of pH = 3.5.

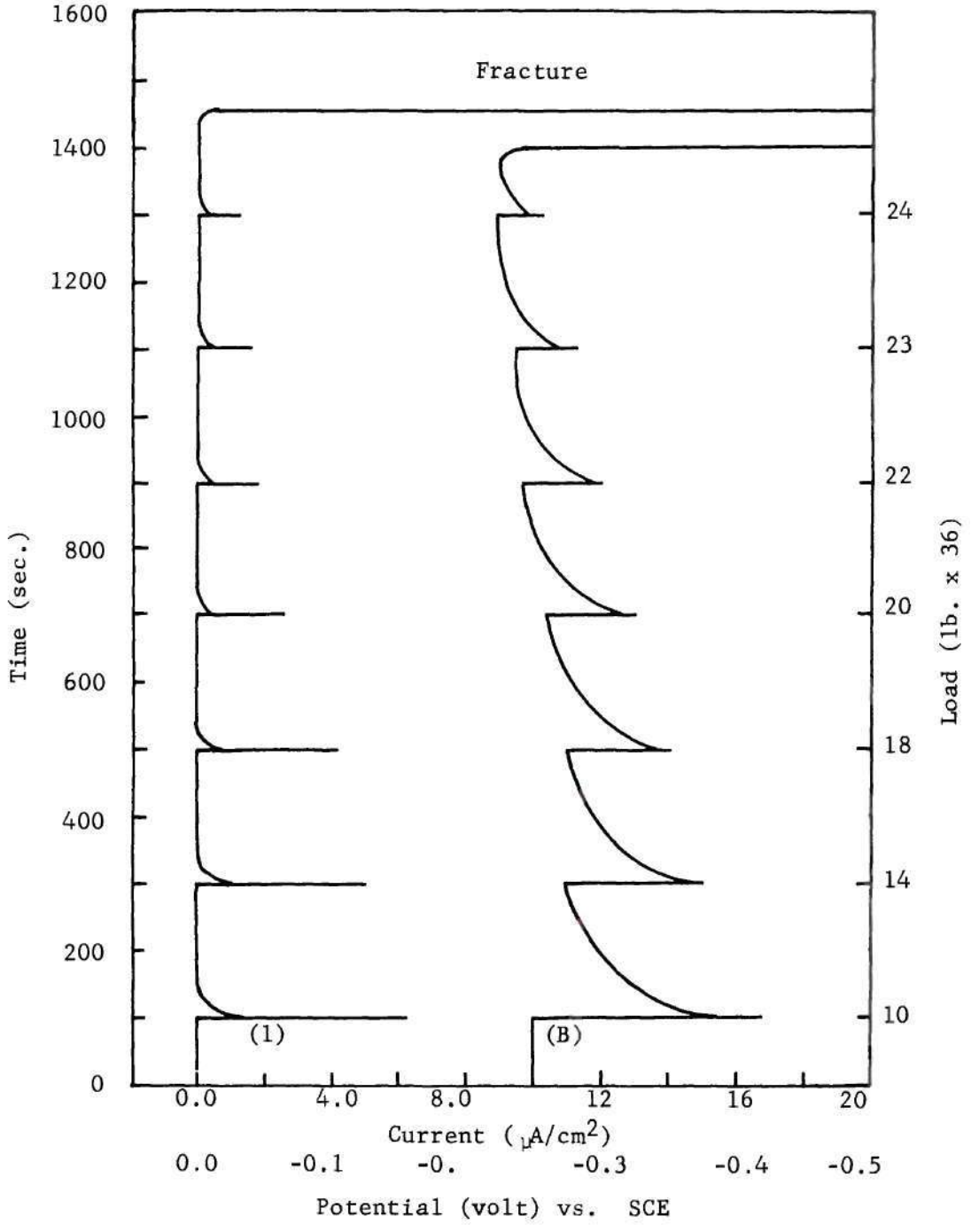

Figure 14. (1) Current vs time and (2) Potential vs Time Curves of the Notched Specimens under Bending in a NaCl Solution with pH = 3.5. Notched Specimens under Tension show the Similar Results.

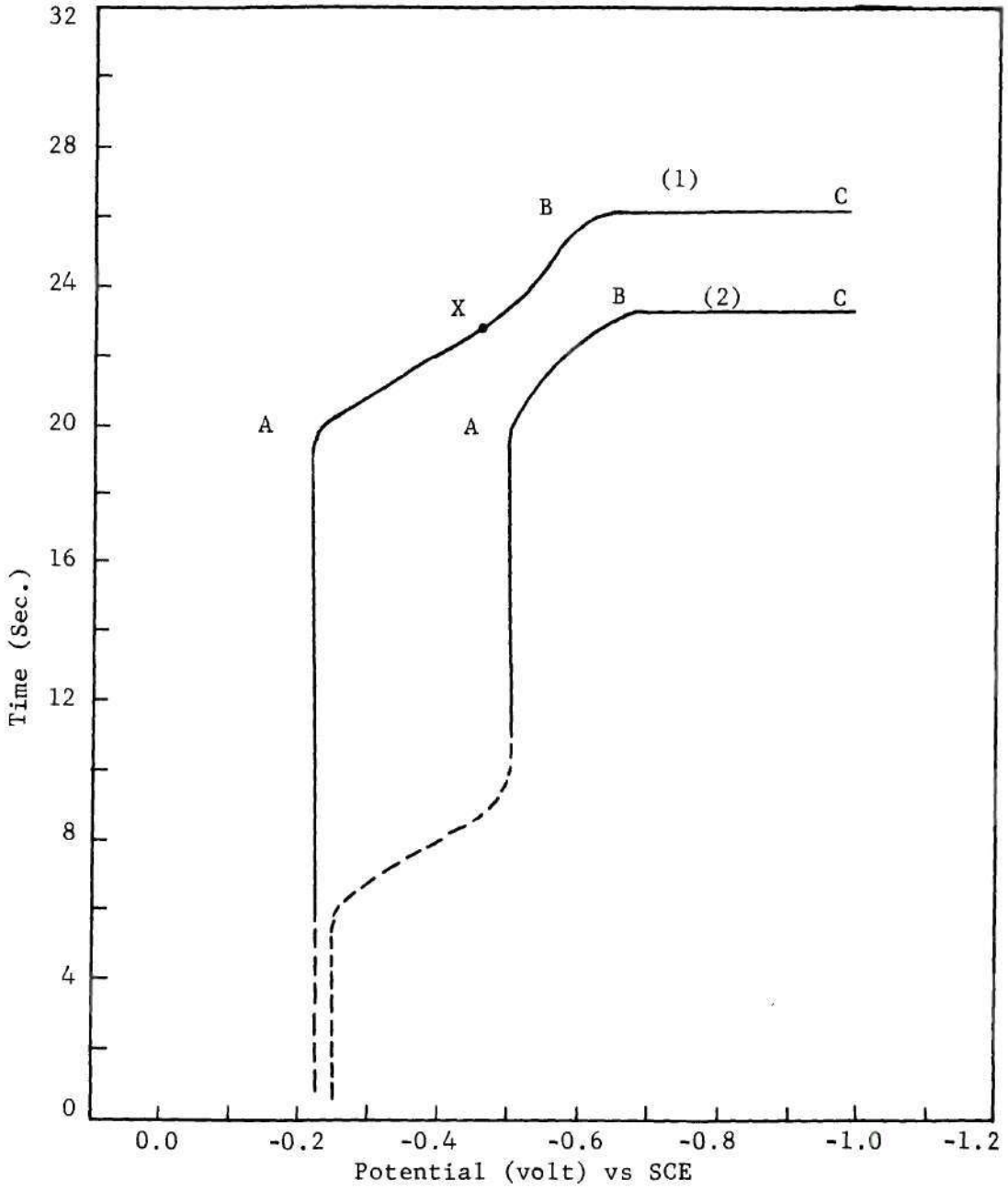

Figure 15. Potential vs Time Curves of the Specimens in a NaCl Solution with pH = 3.5, Using Higher Chart Speed to Determine the Cracking Process, (1) the Bending Specimen, (2) the Tensile Specimen.

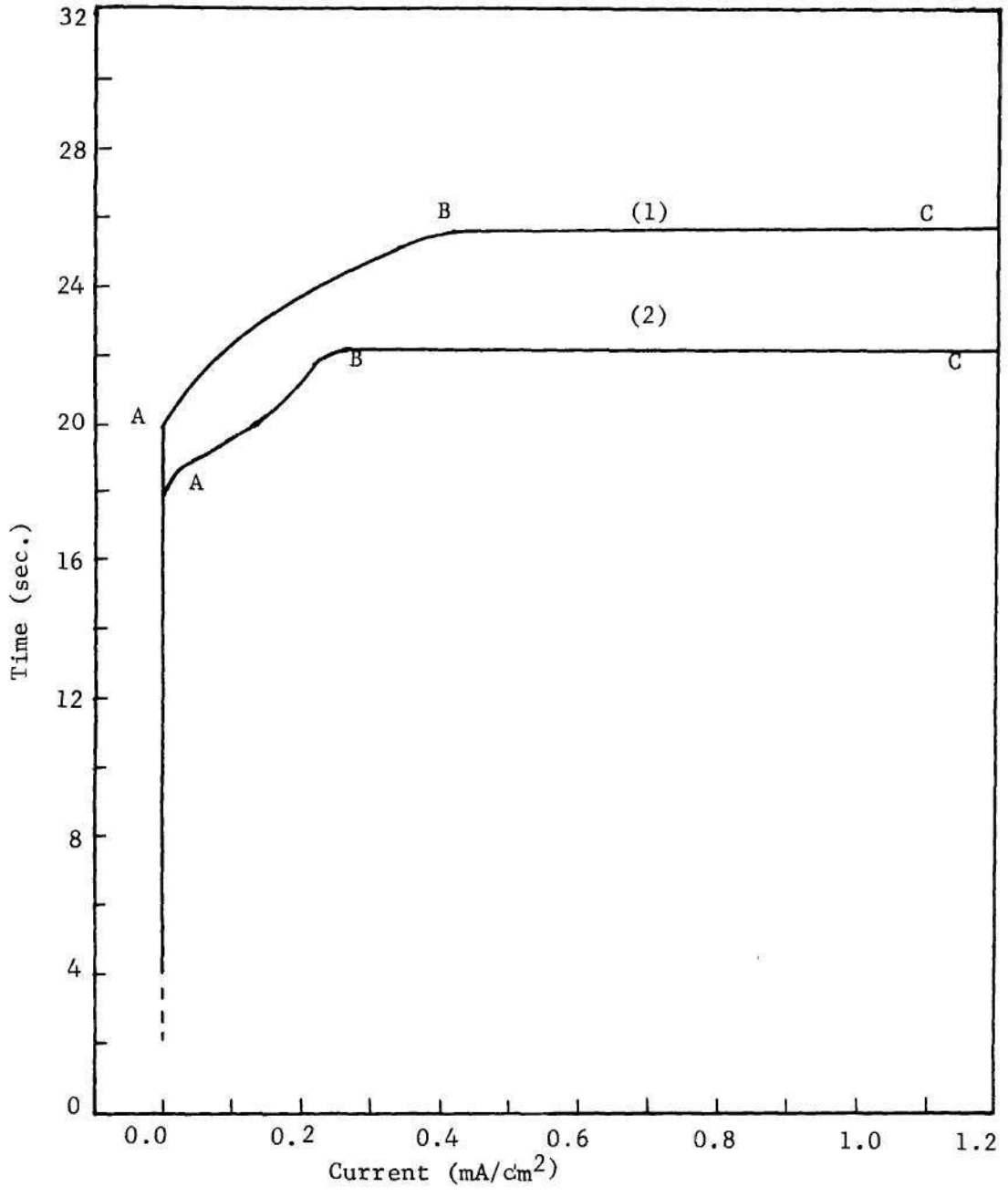

Figure 16. Current vs Time Curves of Specimens in a NaCl Solution with pH = 3.5, Using Higher Chart Speed to Determine the Cracking Process and the Current during Cracking, (1) the Bending Specimen, (2) the Tensile Specimen.

Table 1. Repassivation Power

Solution 3.5%	R.P. volt/min
HCl	0.16
NH_4Cl	0.17
$MgCl_2$	0.18
KCl	0.16
NaCl	0.15
KI	0.25
$NaNO_3$	0.12
HNO_3	0.28
$MgSO_4$	0.22
K_2SO_4	0.16

Table 2. Free Energy Data

Formula	State	Free Energy (Kcal/mole)
Ti	solid	0.00
Cl^-	aqueous	-31.35
$TiCl_2$	solid	-96
$TiCl_3$	solid	-148
$TiCl_4$	liquid	-161.2
$AlCl_3$	solid	-151.2

Table 3. Reaction Potential

Reaction Formula	Free Energy Change (Kcal)	Potential (volt vs SHE)
$Ti + 2Cl^- = TiCl_2 + 2e$	-33.3	0.73
$Ti + 3Cl^- = TiCl_3 + 3e$	-53.95	0.78
$Ti + 4Cl^- = TiCl_4 + 4e$	-35.8	0.39
$Al + 3Cl^- = AlCl_3 + 3e$	-58.2	0.85

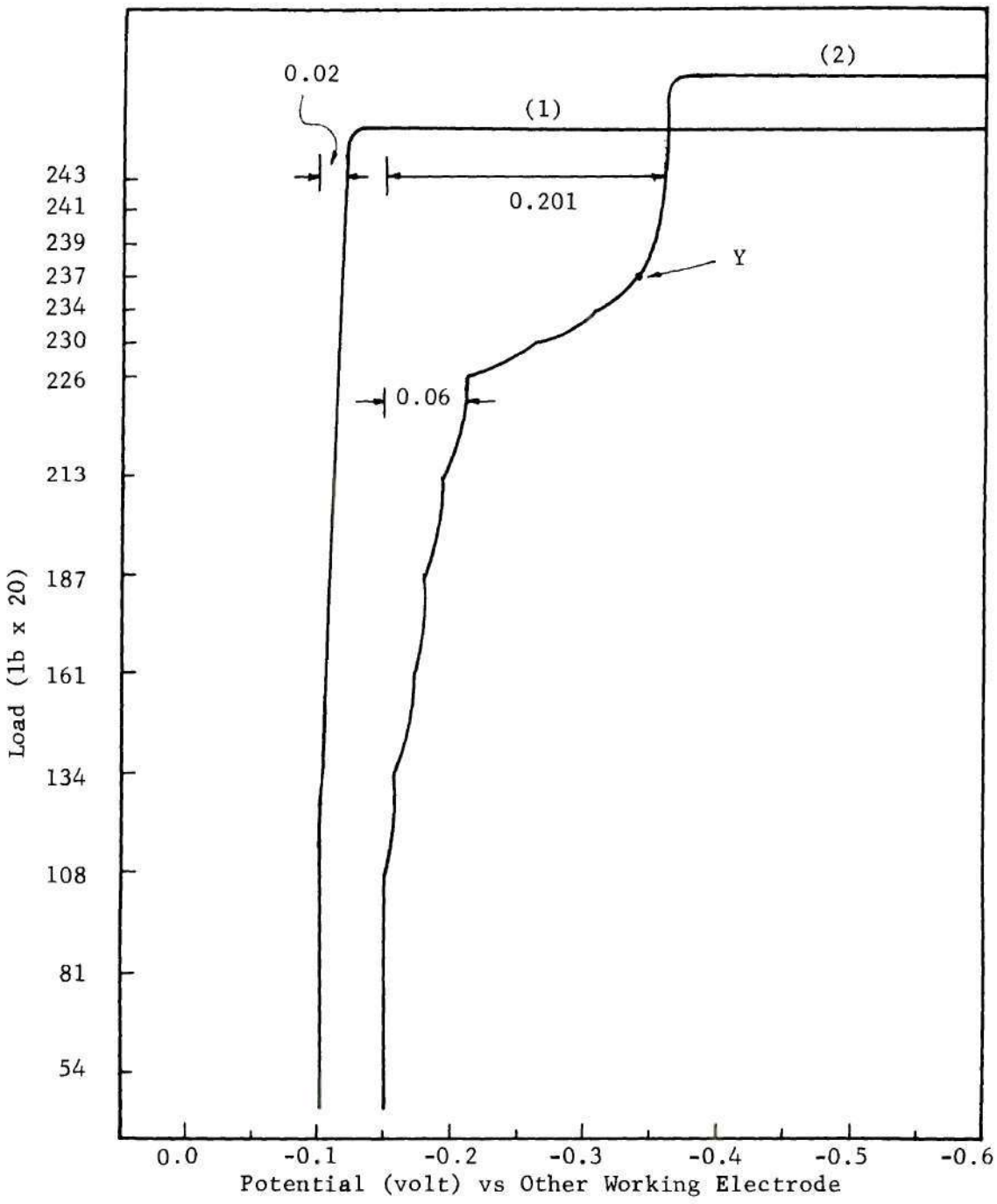

Figure 17. Potential vs Load Curves of Specimens in NaCl Solution with pH = 3.5 under Tension, (1) Using the Special Specimen (Figure 7), (2) Using the Flat Specimen (Figure 6). Load Held Constant after Point Y.

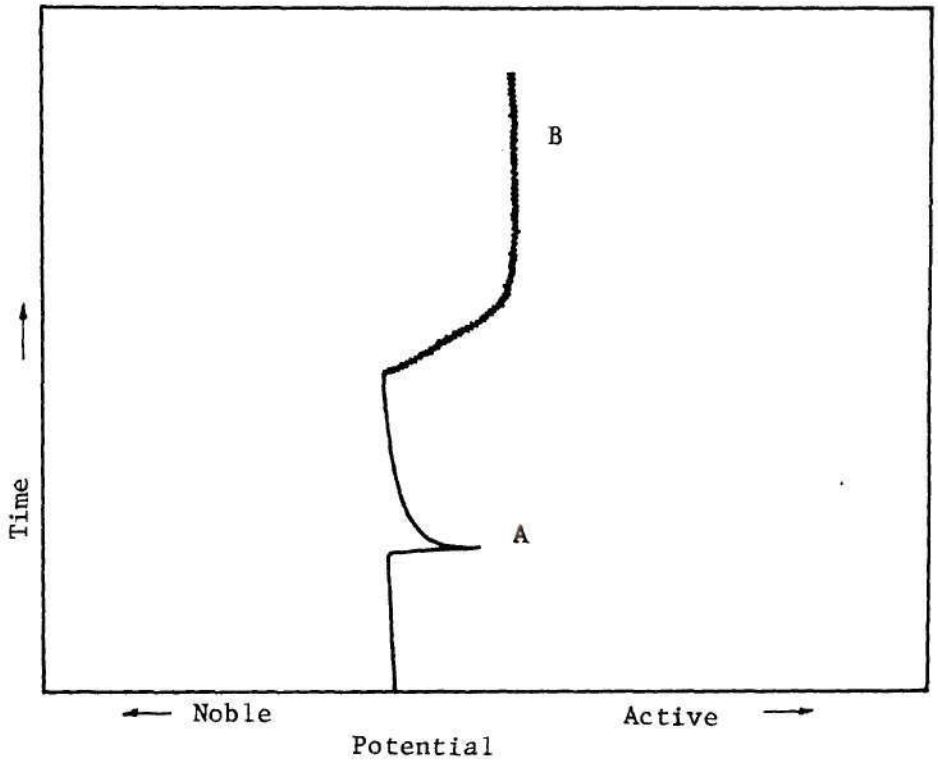

Figure 18. Schematic Curve of Time vs Potential as Affected by Scratching the Specimen, (A) a Large Scratch, (B) Repeatedly Scratching the Surface with Small Scratches.

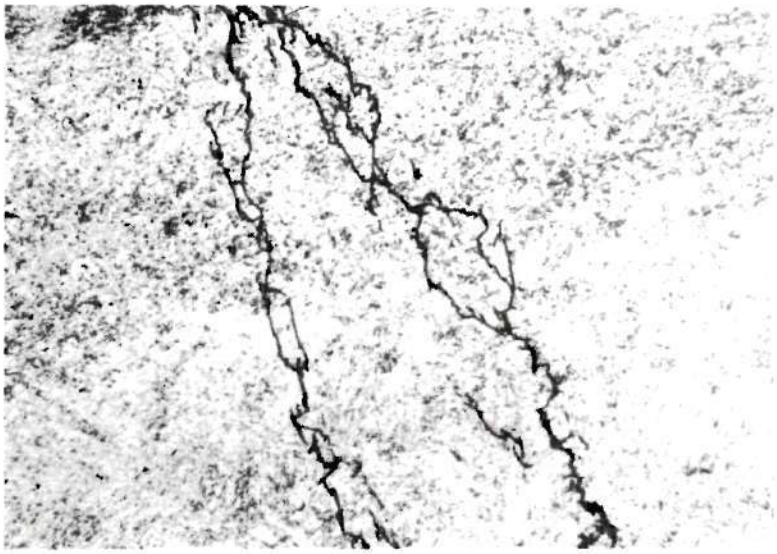

(A)

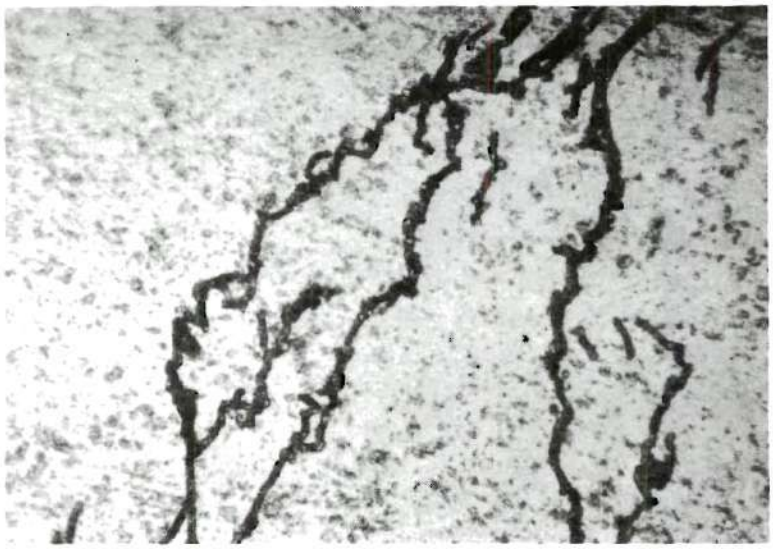

(B)

Figure 19. Microstructure of a Specimen which was bent in NaCl Solution of pH = 3.5 until the Measured Potential Reaching a Point X as shown in Figure 15 was Observed. The unbroken Specimen was Removed from the Solution and then Metallographically Examined, (A) 170 X Magnification, (B) 500 X Magnification. Etchant: 1 part of HF, 1 part of HNO_3 and 2 parts of Glycerine.

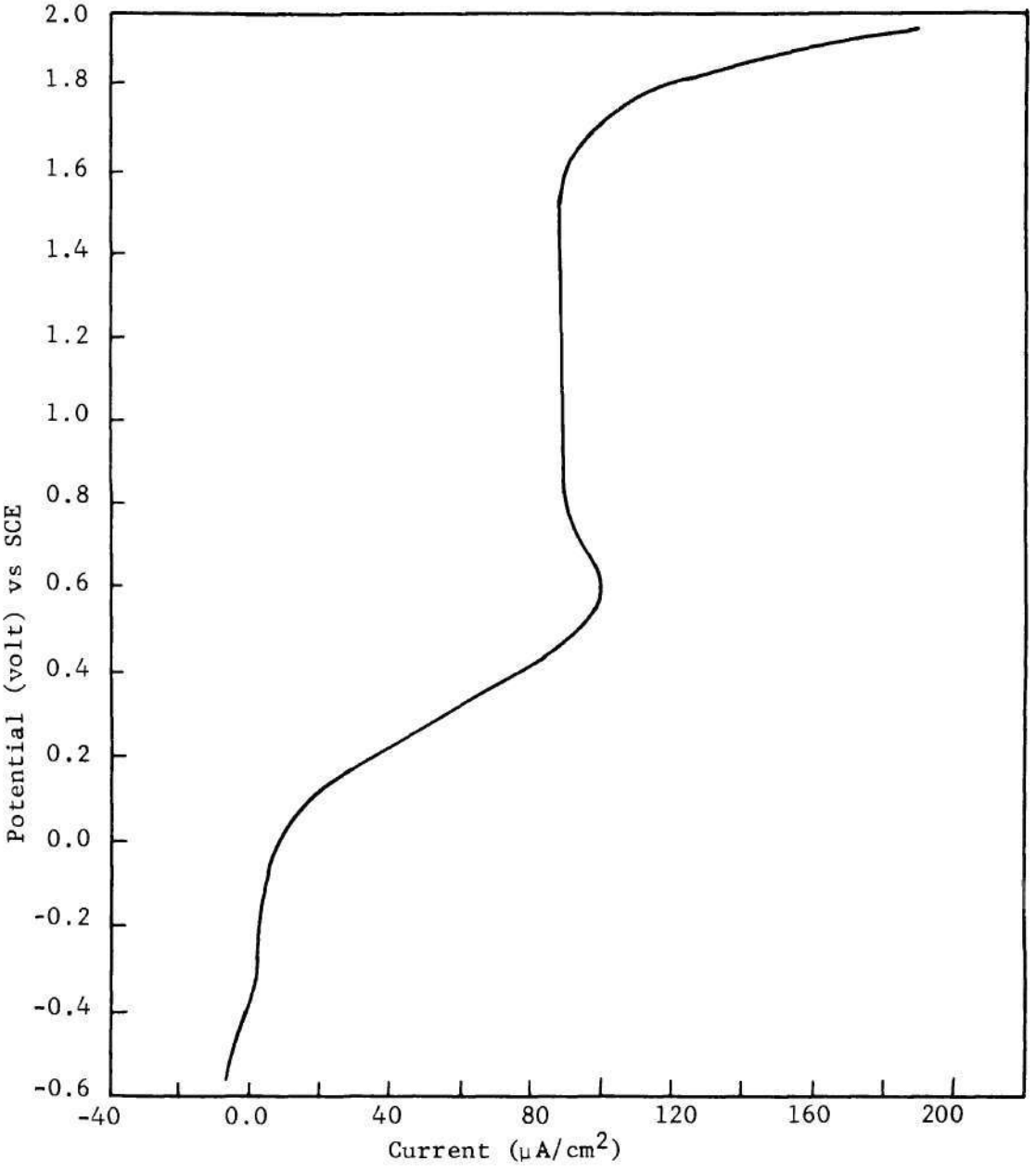

Figure 20. Anodic Polarization Curve of an Unstressed Specimen in a NaCl Solution with pH = 3.5. The Specimen was Polished and Exposed to Air for 23 Hours before Testing.

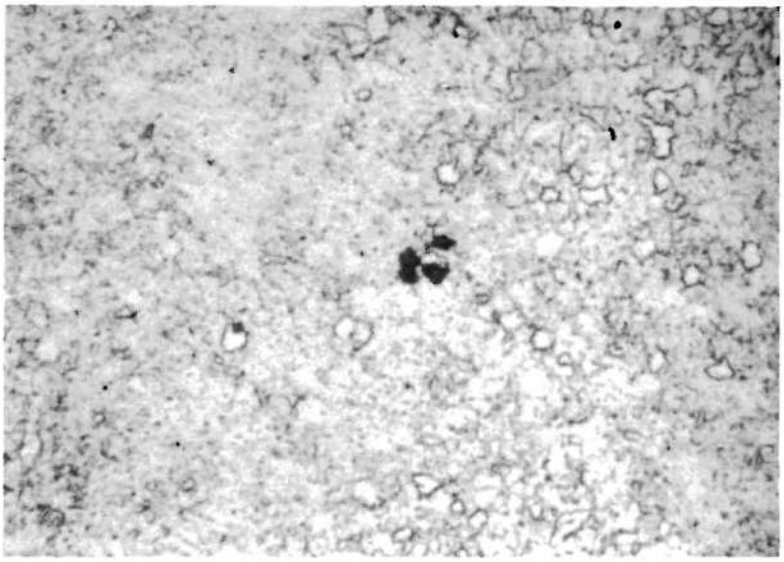

Figure 21. Pitting was Observed on the Surface of an Unstressed Specimen as Potential Changed from 1.6 to 2.0 volt (SCE) in the Anodic Polarization Curve. Pitting Initiates at the Grain Boundaries. 300X Magnification. Etchant: 1 part of HF, 1 part of HNO_3 and 2 parts of Glycerine.

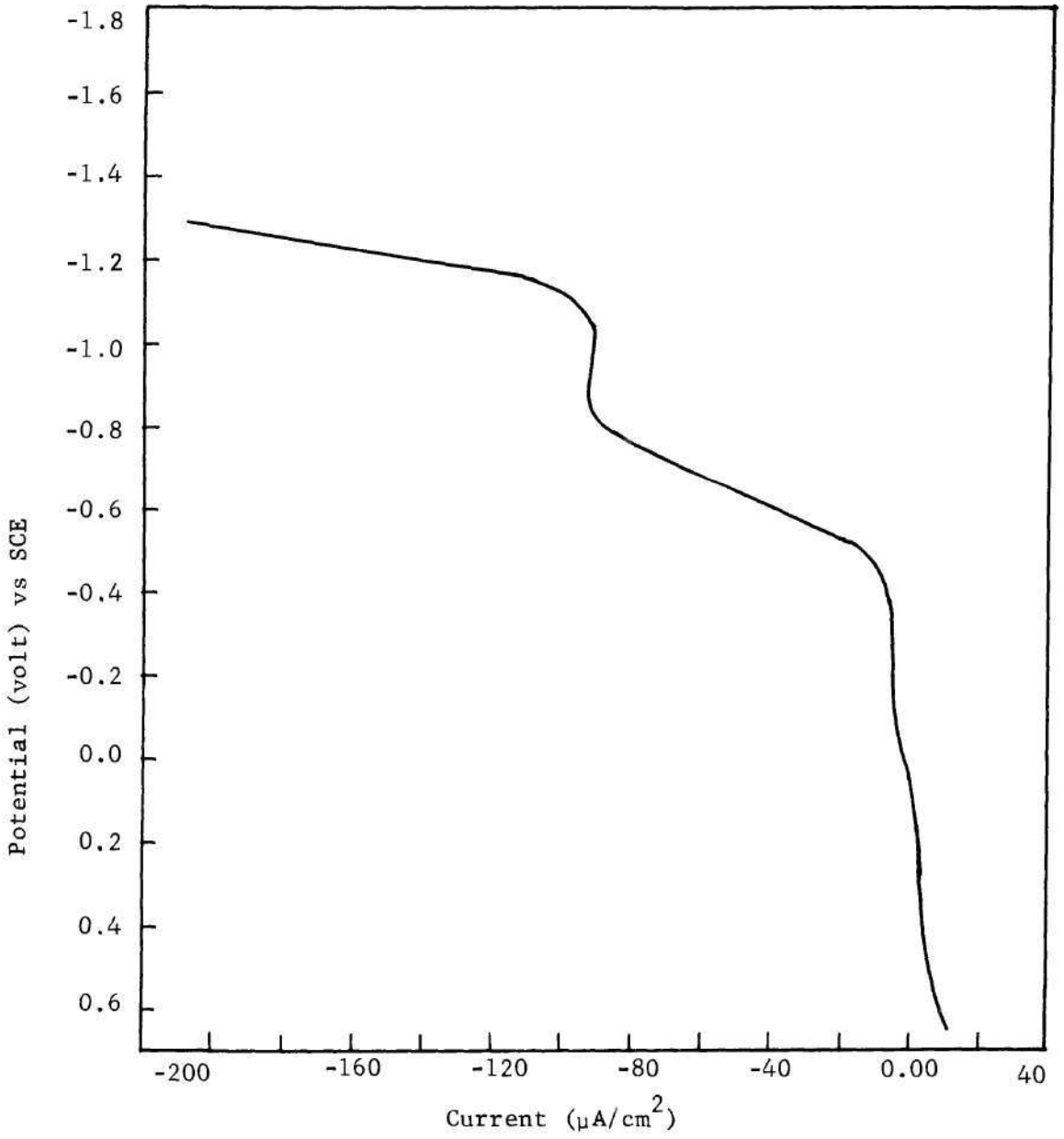

Figure 22. Cathodic Polarization Curve of an Unstressed Specimen in a NaCl Solution with pH = 3.5. Specimen was Polished and Exposed to Air for 20 Hours before Testing.

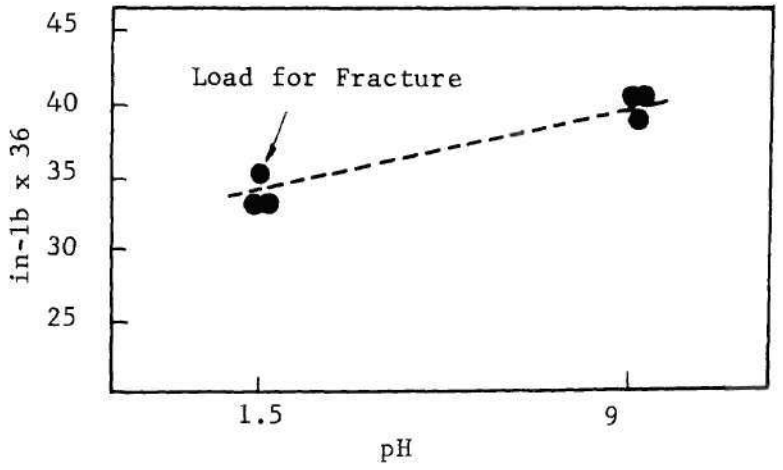

Figure 23. Effect of pH Value on the Stress Corrosion Cracking of Ti:8-1-1 Alloy in 3.5% NaCl Solutions during Bending Tests.

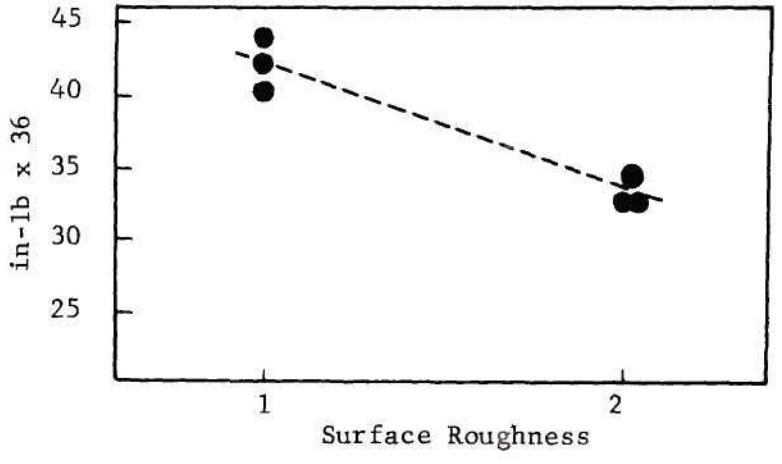

Figure 24. Effect of Surface Roughness on the Stress Corrosion Cracking during Bending Tests in 3.5% NaCl Solution with pH = 3.5, (1) 1Micron Fine Polish, (2) Rough Polish by Bench Grinder.

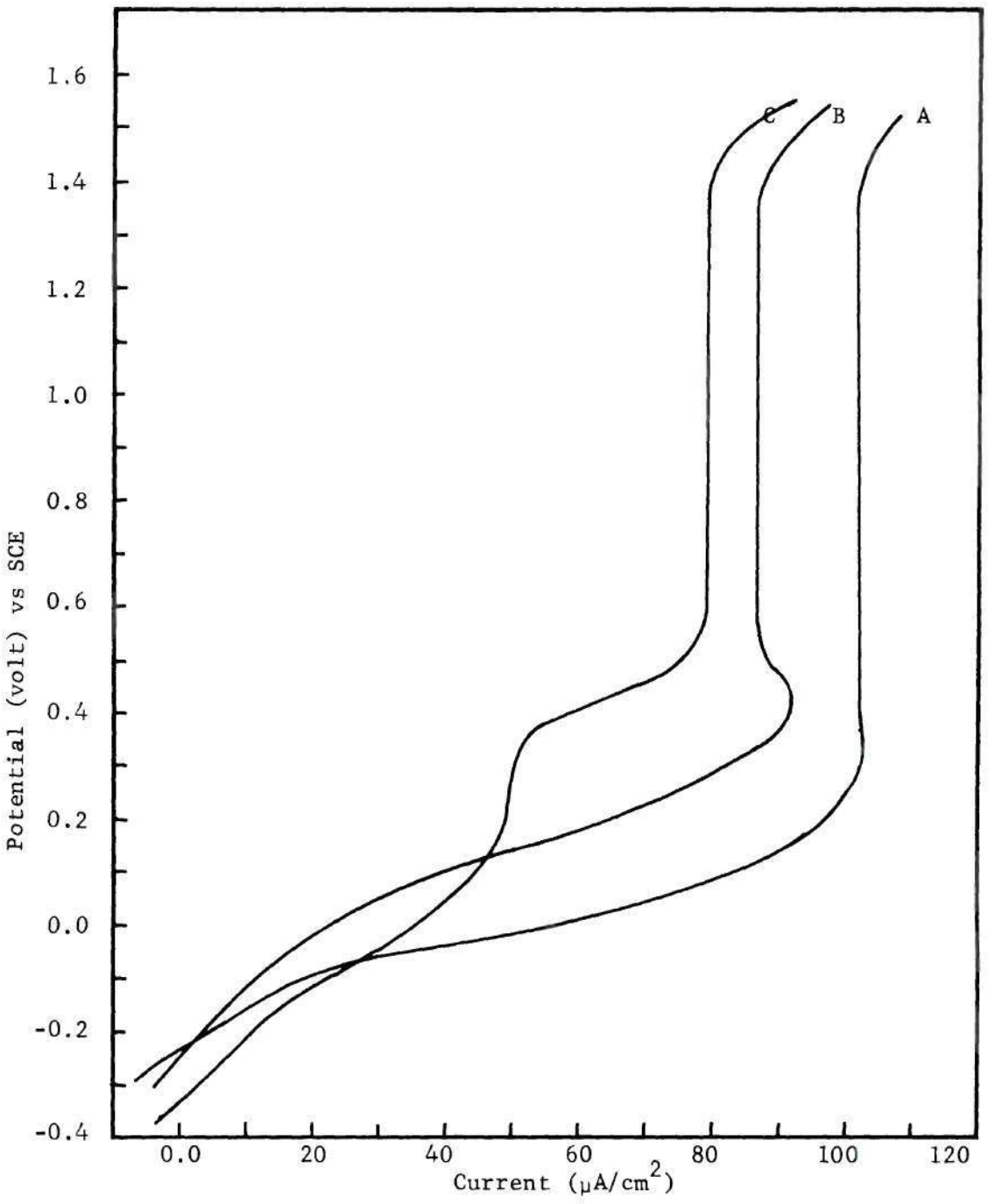

Figure 25. Effect of the pH Value on Anodic Polarization Curves of Unstressed Specimens in a NaCl Solution with pH Equal to (A) 1.5, (B) 5.5 and (C) 8.5.

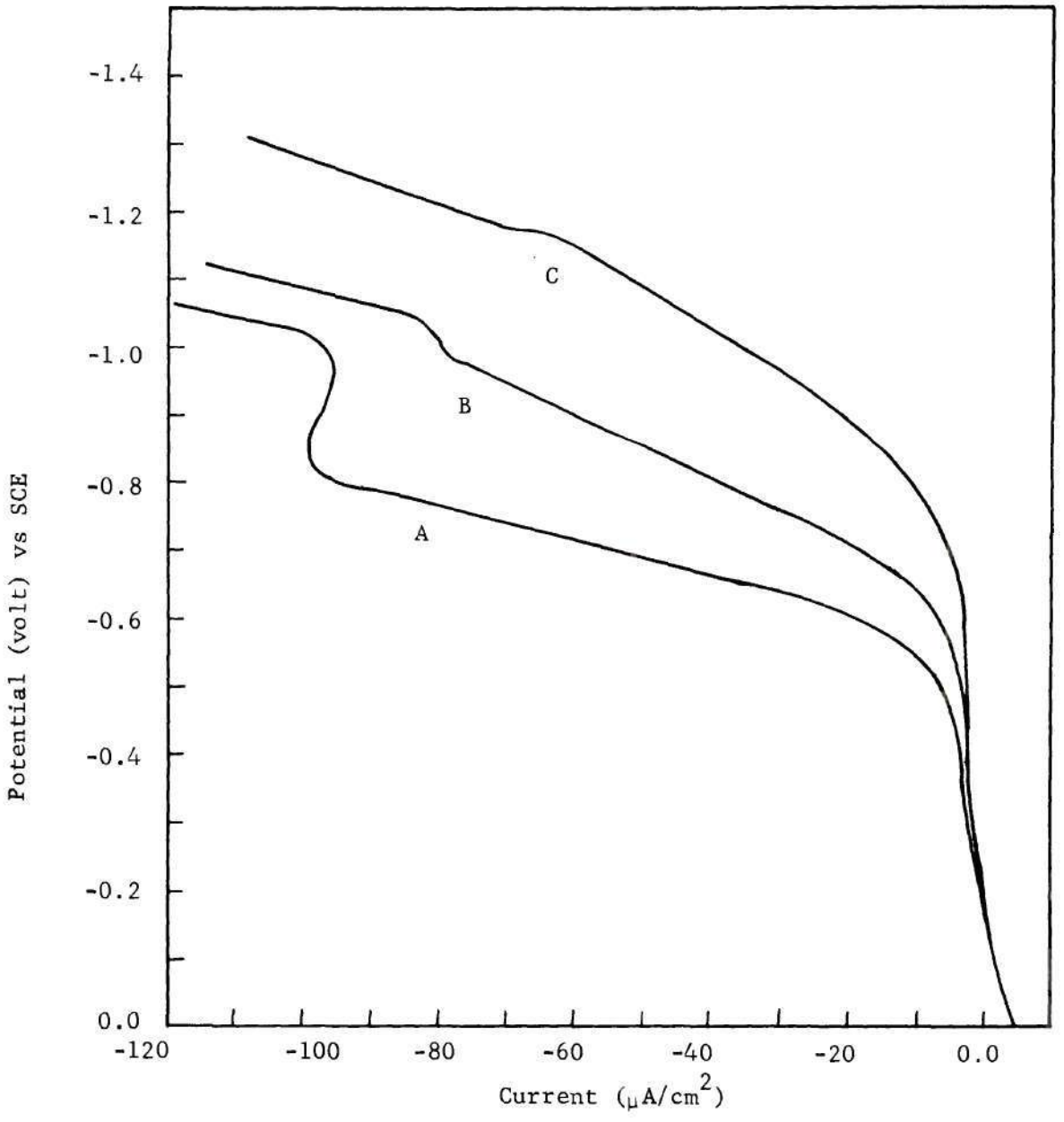

Figure 26. Effect of the pH Value on Cathodic Polarization Curves of Unstressed Specimens in a NaCl Solution with pH Equal to (A) 1.5, (B) 5.5, and (C) 8.5.

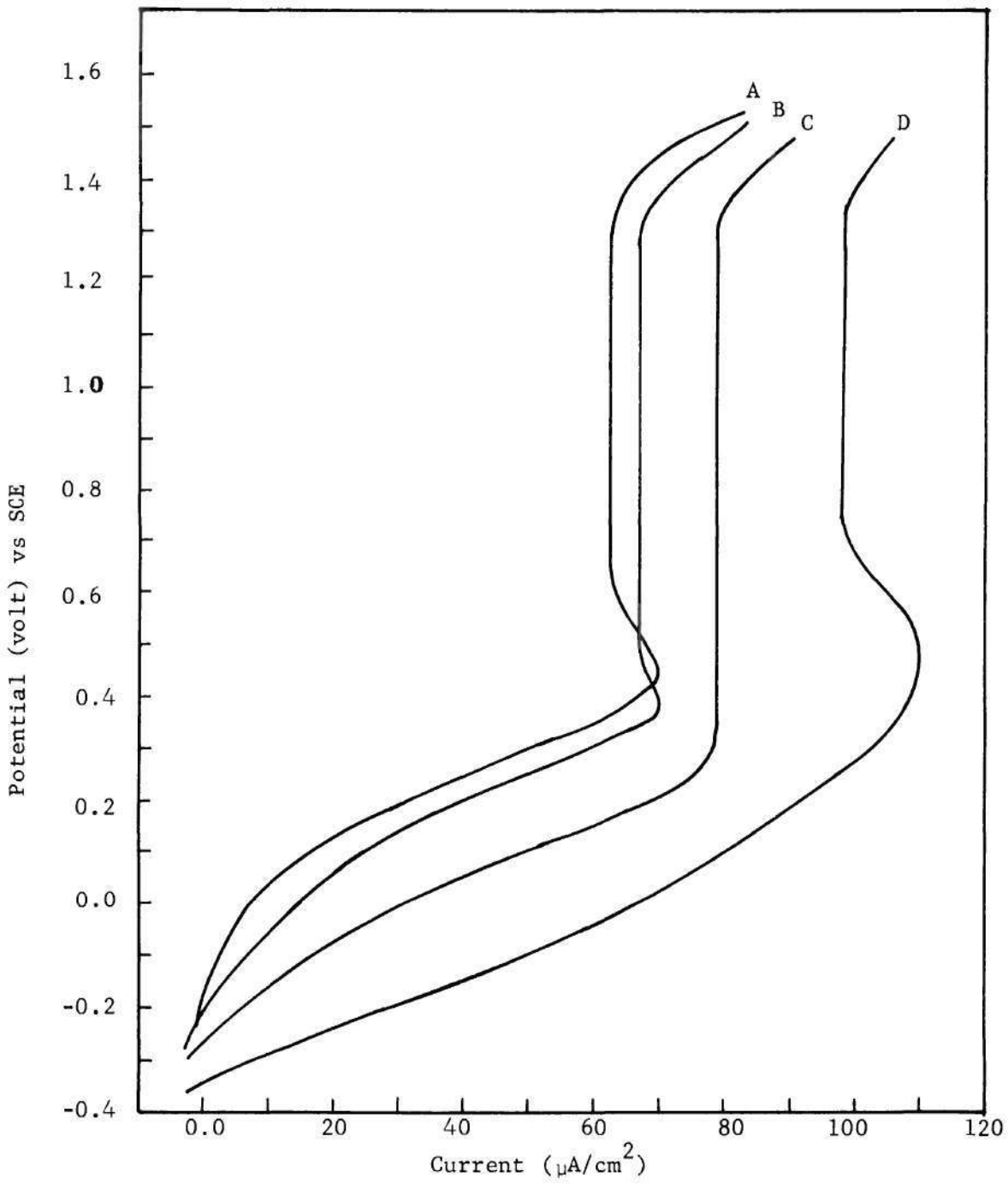

Figure 27. Effect of the Surface Finish on Anodic Polarization Curves of Unstressed Specimens in a NaCl Solution with pH = 3.5. Specimens were Polished and Exposed to Air Before Testing for: (A) 12 hours, (B) 5 hours, (C) 5 minutes and (D) 5 seconds.

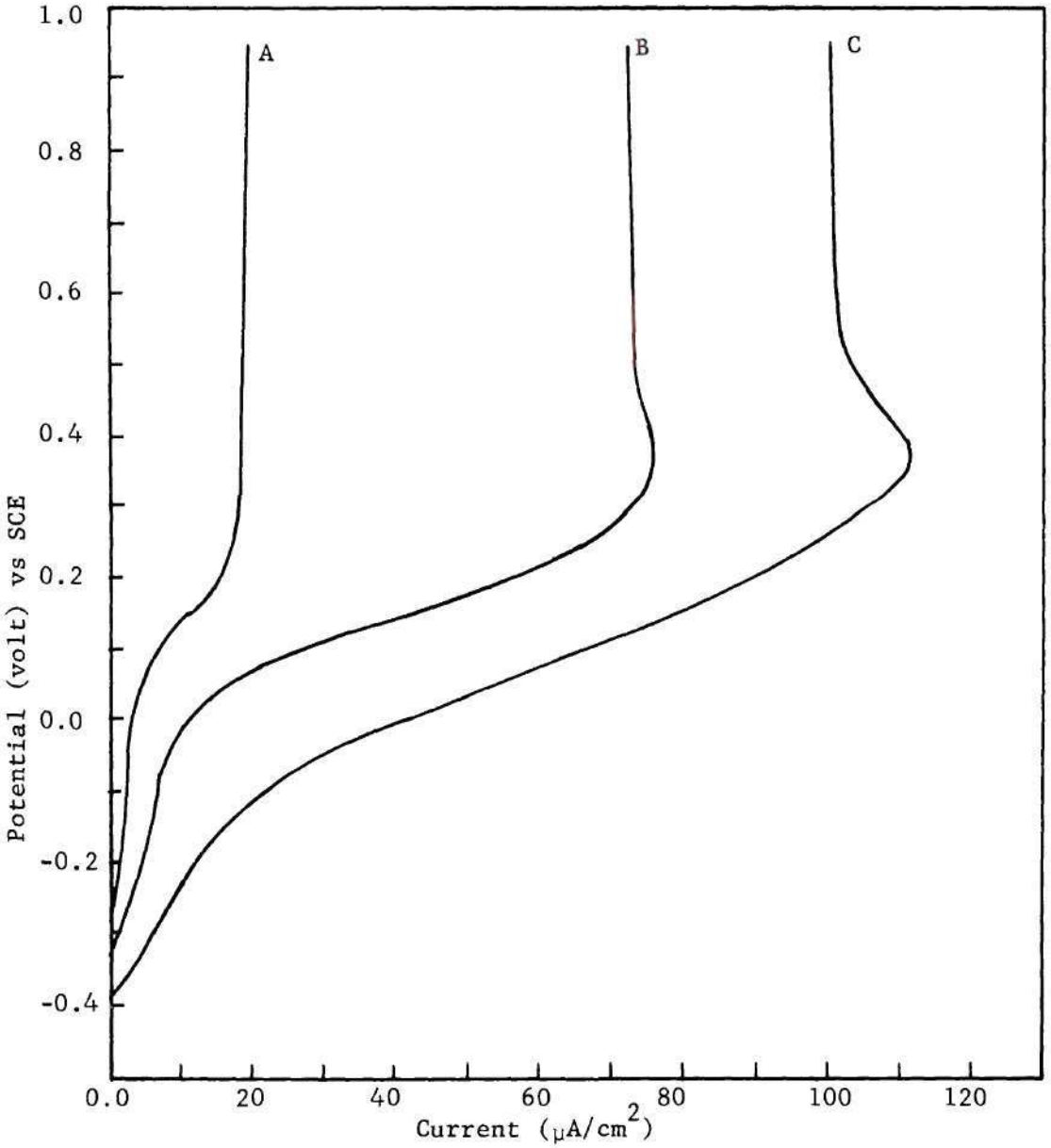

Figure 28. Effect of Surface Finish on Anodic Polarization Curves of Unstressed Specimens in a NaCl Solution with pH = 3.5. (A) 1 Micron Fine Polish, (B) No. 3 Emery Paper Polish and (C) Rough Polish by Bench Grinder.

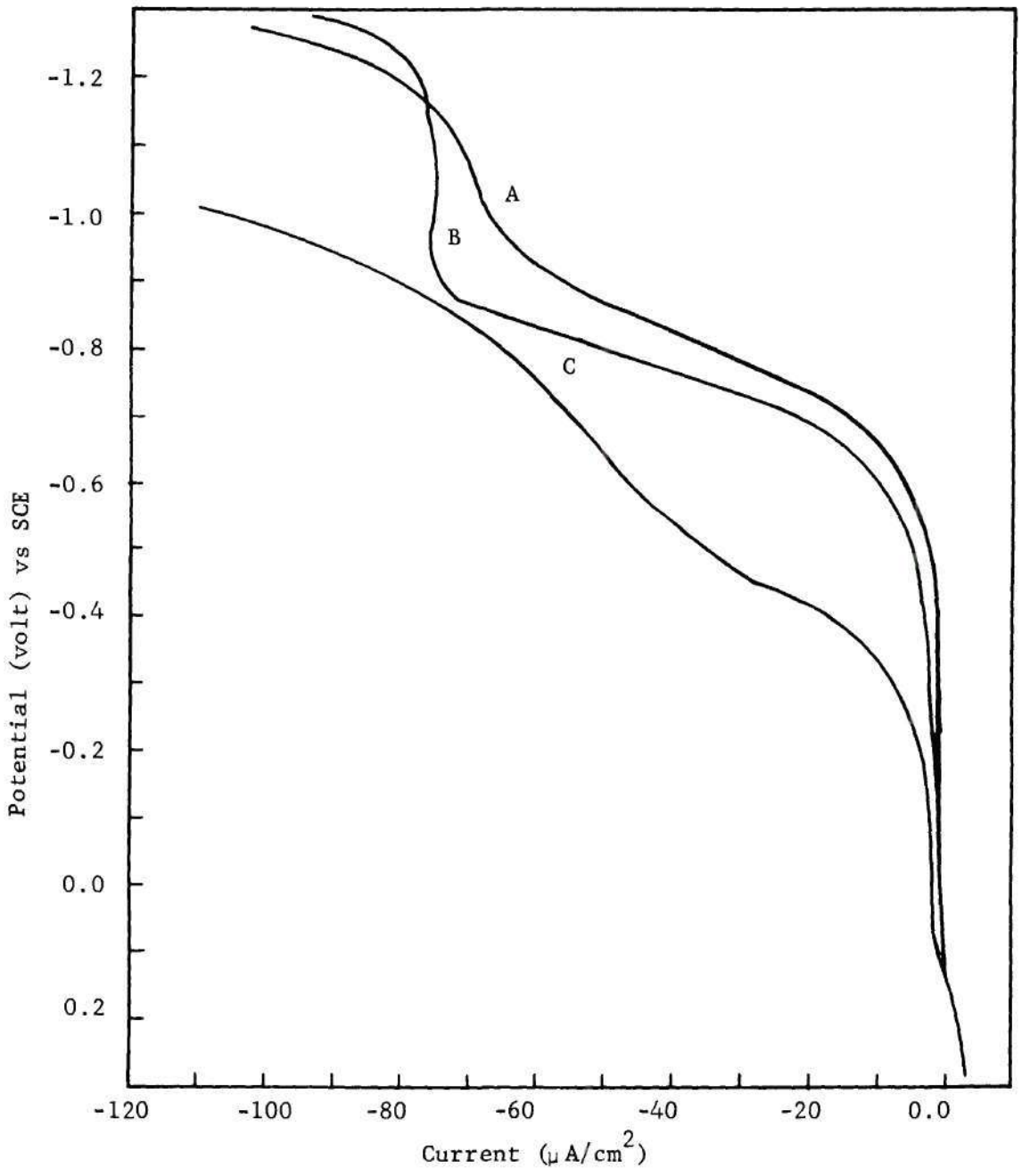

Figure 29. Effect of Surface Finish on the Cathodic Polarization Curves of Unstressed Specimens in a NaCl Solution with pH = 3.5. (A) 1 Micron Fine Polish, (B) No. 3 Emery Paper Polish and (C) Rough Polish by Bench Grinder.

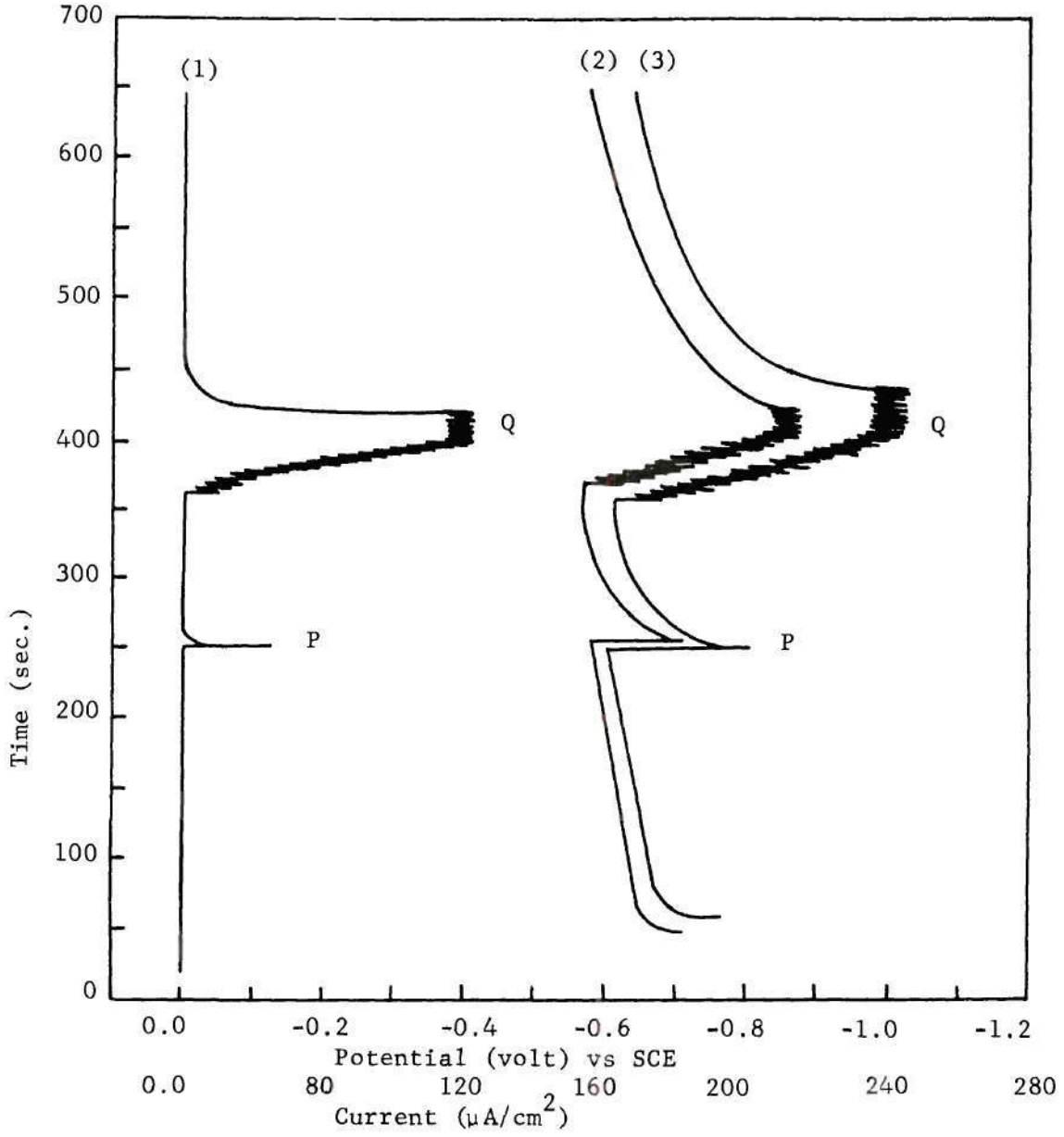

Figure 30. Current and Potential Changes as a Result of Scratching the Surface of the Unstressed Specimens in NaCl Solution, (1) Current vs Time Curve. Potential vs Time Curves in (2) pH = 3.5 and (3) pH = 11.5 Solutions. P is a Curve for one Scratch and Q is a Curve for Numerous Fine Scratches on the Surface.

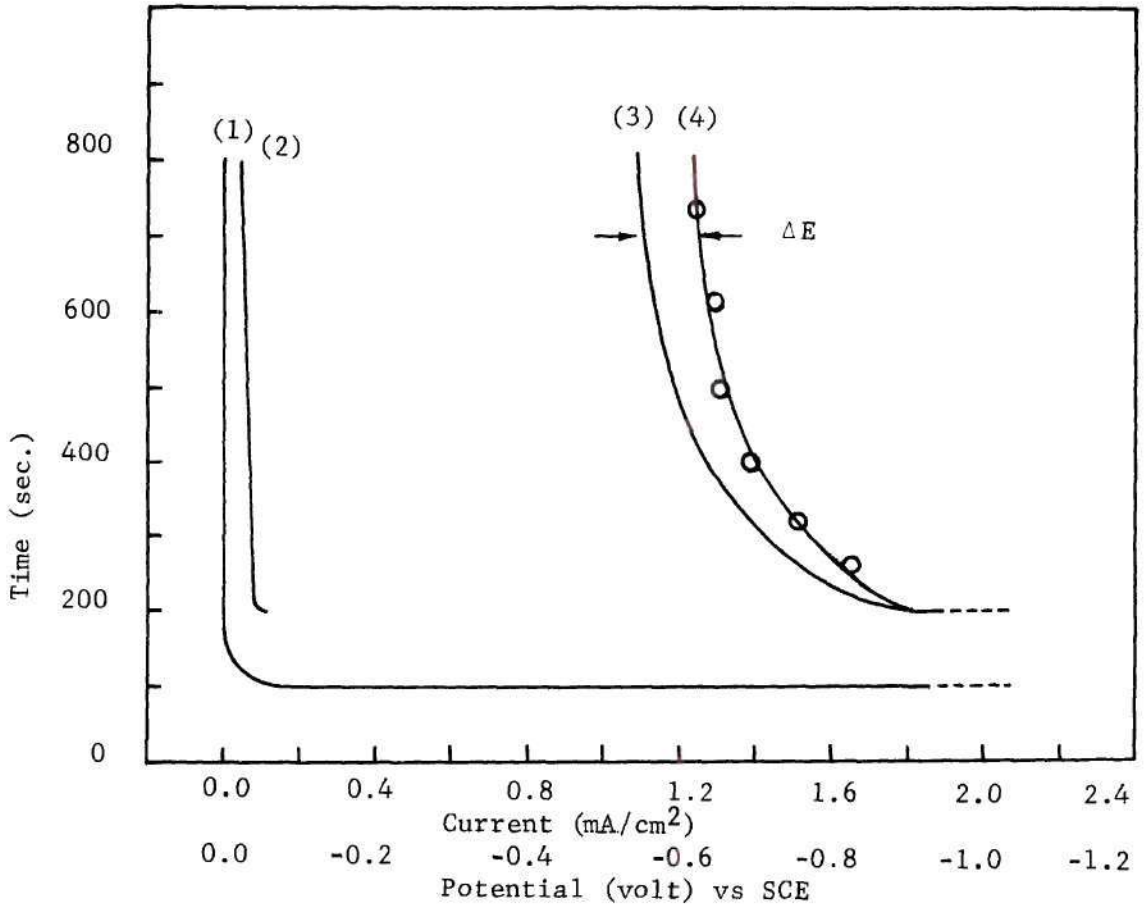

Figure 31. Effect of the Surface Finish on Current and Adsorption Phenomena of Unstressed Specimens, (1) Current between the two Specimens One with a Film-Covered Surface and the other with a Fresh Surface, (2) Potential Curve of a Specimen with Film-Covered Surface, (3) Potential Curve of a specimen with a Fresh Surface, (4) Potential of Specimens When they were Immersed in NaCl Solution After Exposing them to Air for Different Period of Time.

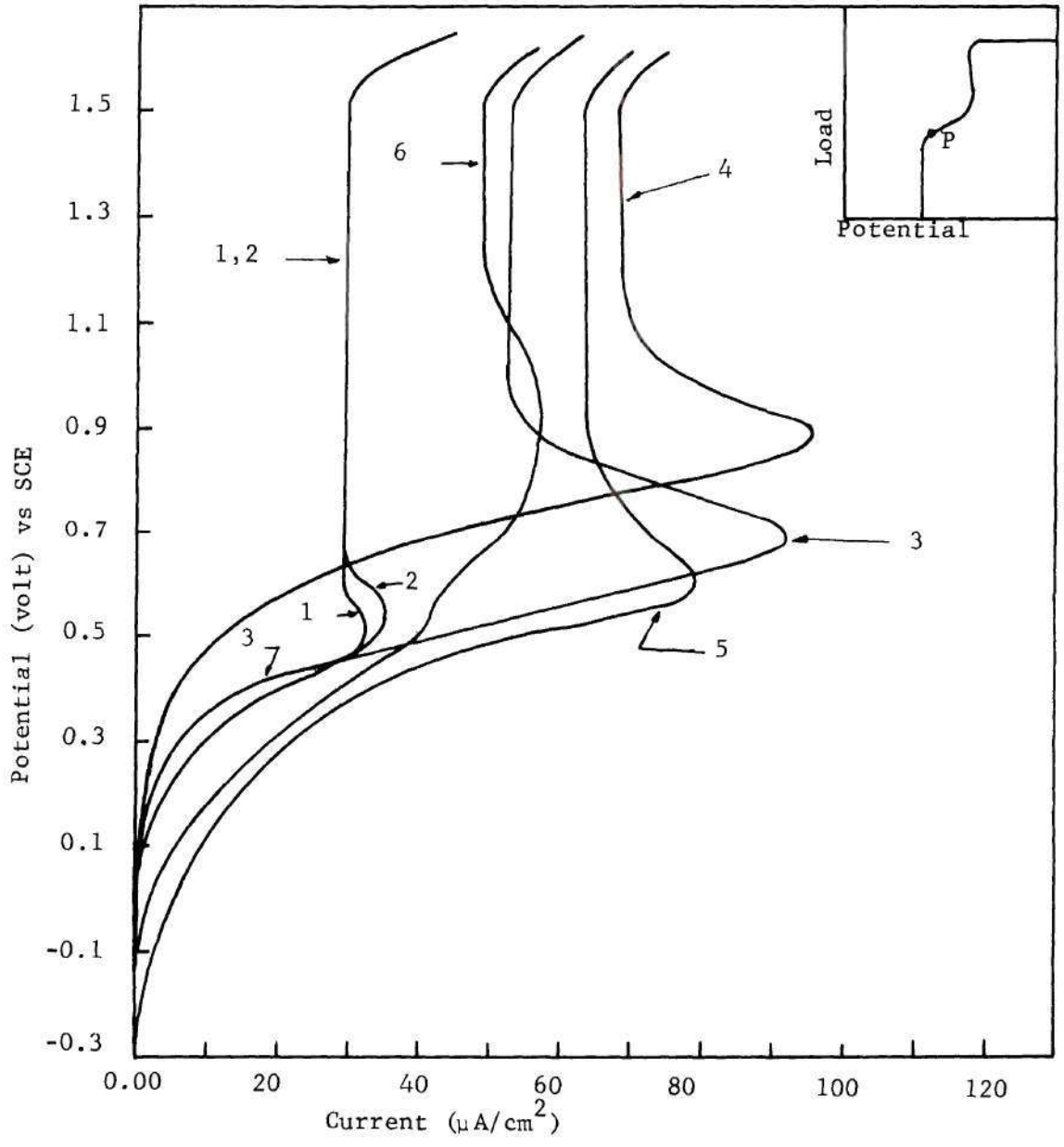

Figure 32. Effect of the Tensile Stress on the Anodic Polarization Curves of Specimens in a NaCl Solution of pH = 3.5, (1) is the Unstressed Specimen, (2) is the Stressed Specimen just below the Point P, (3), (4) and (5) are the Stressed Specimens above the Point P. (6) is the Stressed Specimen above the Point P in 3.5% K_2SO_4 Solution with pH = 3.5, where Point P is at the Yield Point Shown in the Inset in the upper Corner of this Figure.

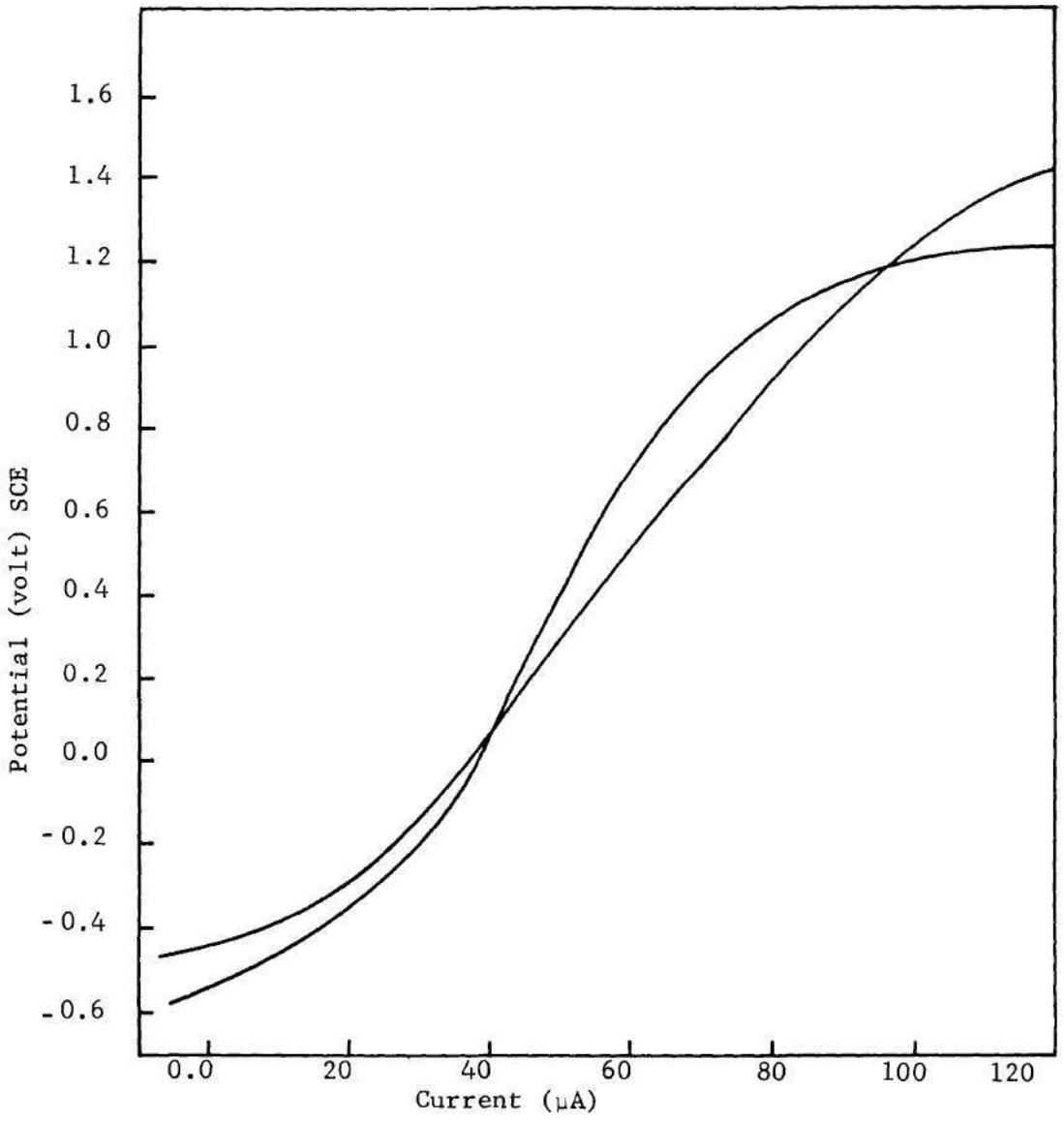

Figure 33. Anodic Polarization Curves of the Bending Specimens during Cracking in NaCl Solution of pH = 5.2.

CHAPTER IV

DISCUSSION OF RESULTS

The Cracking Process

The potential versus time curves in Figure 15 can be divided into four regions which may be correlated with the stress corrosion cracking process: (1) the incubation period below point A, (2) crack initiation at point A, (3) crack propagation between A and B, (4) rapid fracture between B and C.

In the bending tests, no cracks were observed on the surface of the specimen when the sample was removed from the solution before the potential reached point A, Figure 15. This region was then designated as the incubation period. However, cracks were observed when the samples were loaded in the region between A and B, i.e. Figure 19. Therefore, it can be deduced that cracks initiate at point A and propagate until point B is reached. Here catastrophic failure occurred. If the specimens were loaded to a point X located between A and B, and then broken in air, the fracture surface contained two regions, one with cleavage and the other with ductile fracture. The cleavage occurred in solution during the crack propagation period from A to X, and ductile fracture occurred when the specimen was broken in air after being removed from the solution. The cleavage area on the fracture surface increased with increasing time from A to X. The region between A and B in the potential and the current versus time curves shown in

Figures 15 and 16 is continuous. This indicated the crack propagation was continuous.

The same phenomenon was observed in tensile tests. However, potential and current changes were observed before point A as shown in Figures 12 and 15. No cracks were observed under the microscope when the specimen was removed from the solution before the potential reached point A; and no cleavage region could be found on the fracture surface of a sample which was not loaded above point A and then broken in air. This supports the conclusion that cracks did not initiate below point A, and that the current generated below point A (Figure 12) did not change the characteristics of the fracture.

Effects of Surface Conditions on Potential and Adsorption

The shift in the potential towards the active direction can not be explained by the change in strain energy and the thermoeleastic effect. A quantitative calculation of the potential change from the strain energy and thermoeleastic effect is about 0.01 mV. The experimental value obtained from Figure 17 is about 0.06 volt. The potential change may be due to the change in the surface condition. A special sample was designed (Figure 7) which contained about the same strain energy as the regular sample (Figure 6) when loaded. Its measured potential change was very small in comparison with the regular specimen. This is shown in Figure 17. This is attributed to the difference in stress at the section of measurement which affects the surface condition. Support for this interpretation was obtained by scratching the surface of an unloaded specimen in the solution. The measured potential change was found to be very similar to that of the specimen loaded beyond the yield point (Figure 18).

Therefore, the potential changes of specimens when stressed above the yield point in NaCl solutions is due to film-rupture. The notched specimens showed a sharp change in potential and current as an incremental load was added (see Figure 14). This may be due to the notch acting as a stress raiser or concentrator. Dislocations and local microslip created around the root of the notch make it much easier to rupture the passive oxide film which results in exposure of the fresh surface to the corroding media. The exposed surface is then repassivated.

The potential difference, ΔE, between curve (3) and curve (4) in Figure 31 can be considered to be due to the adsorption of ions from the solution on the metal surface, making the assumption that the growth of the oxide film on the metal surface occurs at approximately the same velocity in air as in the solution. The adsorption may decrease the surface energy and/or form an adsorption layer which changes the potential. This figure also indicates that the film-covered surface has lower adsorption characteristics (curve 2) than the fresh surface (curve 3). This implies that the decrease of surface energy is an important factor in crack propagation. Its role in crack initiation appears to be much less if indeed it effects initiation at all.

Anodic Dissolution

There is very little active region in the anodic polarization curves for specimens stressed to the yield point in NaCl solutions or stressed beyond the yield point in a K_2SO_4 solution (Figure 32).

However, a large active region is exhibited in the anodic polarization curves of specimens stressed beyond the yield point in NaCl solutions, i.e. curves 3, 4, and 5 in Figure 32. This large active region indicates that the anodic dissolution may be responsible for crack initiation.

The fracture of specimens which were scratched during the tensile test in a NaCl solution did not occur in the scratched area. The ruptured film was repassivated in the NaCl solution. Although film-rupture may be necessary for crack initiation it is not a sufficient criterion. Crack initiation may be caused by dislocations piling up against the grain boundaries or other barriers close to the surface, or against the oxide film. The high strain field in the region of the pile-ups may cause serious distortion of metal and surface film. Anodic dissolution may start at that point and dislocations may run out to the surface and assist in the formation of a crack tip.

The electrochemical reactions during crack propagation can be elucidated by anodic polarization behavior during cracking. The anodic polarization was measured after removing the load from the specimen at point X during crack propagation which was about -0.6 volts (SCE) in the potential curve as shown in Figure 15. The anodic polarization curves of Figure 33 may explain crack propagation which involves anodic dissolution. No passive region is observed and the corrosion current increases with increasing potential. This result has been confirmed by Beck (52) who indicated the rate of crack propagation during stress corrosion cracking is linearly related to the potential. This implies that anodic dissolution occurs and plays some part in crack propagation. Anodic dissolution has also been confirmed by Brown (53) who indicated

that aluminum dissolved in solution at the crack tip. Purple spots found at that area indicated a trace of dissolved titanium. Beck (54) suggested that crack propagation may involve the dissolution of titanium. Further support for the dissolution of titanium and aluminum during crack propagation are the low pH value at the crack tip (53), which is about 1.7, and the drop in potential towards the active direction (see Figures 11, 13 and 15). These results are in accordance with the Pourbaix diagram (55). However, the amount of the metal dissolved has never been quantitatively determined.

The negative chloride ions are adsorbed electrically at the anodic crack tip. This adsorption may decrease the surface energy (6) and/or lower the binding energy of the unbroken atomic bonds defining the crack tip (56). The decrease of pH value at the crack tip and on the rough surface of the crack walls favoring the discharge of hydrogen ions has been discussed. The hydrogen atoms may be adsorbed and/or absorbed by the metal and precipitate as hydride phase within the plastic zone (7). However, no hydrides have ever been identified directly on the fracture surface after stress corrosion tests in the NaCl solution. The function of hydrogen in stress corrosion cracking of titanium alloys in NaCl solutions is still not clear.

CHAPTER V

CONCLUSIONS

1. The current density between a fresh surface and a normal air exposed surface is about 2 mA/cm^2. The electrode potential of Ti:8-1-1 alloy with a fresh surface is dependent on the pH value, i.e. -0.88 and -1.02 volt (SCE) in NaCl solution with pH = 3.5 and 11.5 respectively.

2. The results of the experimental work indicate that crack initiation may involve preferential dissolution at the point of dislocation pile-ups; and anodic dissolution at the crack tip is possible and may play some part in crack propagation.

3. A region in the potential and the current versus time curves was directly related to crack propagation and indicated that crack propagation was continuous.

BIBLIOGRAPHY

1. H. H. Uhlig, "An Evaluation of Stress Corrosion Cracking Mechanism," Paper Presented at the Conference on the Fundamental Aspects of Stress Corrosion Cracking. Columbus, Ohio, September, 1967.

2. H. L. Logan, "Stress Corrosion Cracking of Metals," John Wiley and Sons, Inc., New York, 1967.

3. H. W. Picking and P. R. Wann, "Relationship of Heat Treatment and Microstructure to Corrosion Resistance in Wrought Ni-Cr-Mo Alloys," Corrosion, Vol. 19, 375t, 1963.

4. H. H. Uhlig, "Physical Metallurgy of Stress Corrosion Fracture," Edited by T. N. Rhodin, Interscience, New York, 1959.

5. H. H. Uhlig and J. Sava, "Effect of Heat Treatment on Stress Corrosion Cracking of Iron and Mild Steel," Trans. ASM, 56, 361, 1963.

6. E. G. Coleman, E. Weinstein and W. Rostoker, "On a Surface Energy Mechanism for Stress Corrosion Cracking," ACTA Met. 5, 491, 1961.

7. G. Sanderson, D. T. Powell and J. C. Scully, "The Stress Corrosion Cracking of Ti Alloys in Aqueous Chloride Solution at Room Temperature," Corrosion Science, Vol. 8, 473, 1968.

8. V. A. Livanov, J. A. Bukhanova and B. A. Kolachev, "Hydrogen in Titanium," Translated from Russian by A. Aladjem, Chem. Eng. Israel Program for Scientific Translations, 1965.

9. N. A. Tiner, T. L. Mackay, S. K. Asumnaa and R. G. Ingersoll, "Use of Electron Microautoradiography for Evaluation Microsegregation of Hydrogen in Titanium Alloys," Trans. ASM. Vol. 61, 195, 1968.

10. T. R. P. Gibb and H. W. Kruschwitz, "The Titanium-Hydrogen System and Titanium Hydride," J. Amer. Chem. Soc. Vol. 72, pt. 3, 5365, 1950.

11. L. D. Jaffee, "Metallurgraphic Identification and Crystal Symmetry of Titanium Hydride," J. Metals, Vol. 8, No. 7, 1965.

12. T. S. Liu and Morris A. Steinberg, "The Mode of Hydride Precipitation in α-Ti and α-Ti Alloys," Trans. ASM. Vol. 50, 1958.

13. T. P. Papazoglon and M. T. Hepworth, "The Diffusion of Hydrogen in Titanium," Trans. AIME. Vol. 242, 628, 1968.

14. R. J. Wasilewski and G. L. Kehl, "The Diffusion of Hydrogen in Titanium," Metallurgia. Vol. 50, 225, 1954.

15. D. N. Williams, "The Hydrogen Embrittlement of Titanium Alloys," Journal of the Institute of Metals, Vol. 91, 147, 1962-1963.

16. L. W. Berger, D. N. Williams and J. I. Jaffee, "Hydrogen in Titanium-Aluminum Alloy," Trans. AIME. 509, August, 1950.

17. M. R. Louthan, Jr. "Stress Orientation of Titanium Hydride in Titanium," Trans. AIME. Vol. 227, 1166, 1963.

18. David A. Mauney and E. A. Starke, Jr., "Explanation of the Cleavage Plane in Stress Corrosion Cracking of Alpha Phase Titanium-Aluminum Alloys," Corrosion, Vol. 25, No. 4, 1969.

19. R. I. Jaffee, G. A. Lenning and C. M. Crarghead, "Effect of Hydrogen on Alpha Titanium Alloys," J. Metals, Vol. 8, No. 11, 1956.

20. D. N. Fager and W. F. Spurr, "Some Characteristics of Aqueous Stress Corrosion in Titanium Alloys," Trans. ASM. Vol. 61, 283, 1968.

21. M. J. Blackburn and J. C. Williams, "Strength, Deformation Modes and Fracture in Titanium-Aluminum Alloys," Trans. ASM. Vol. 62, 398, 1969.

22. R. E. Curtis, R. R. Boyer and J. C. Williams, "Relationship between Composition, Microstructure and Stress Corrosion Cracking (in Salt Solution) in Titanium Alloys," Trans. ASM. Vol. 62, 475, 1968.

23. R. E. Curtis and W. F. Spurr, "Effect of Microstructure on the Fracture Properties of Titanium Alloys in Air and Salt Solution," Trans. ASM. Vol. 61, 115, 1968.

24. Sanderson and J. C. Scully, "Hydride Formation in Corroded Titanium Alloys," Corrosion Science , Vol. 6, 541, 1966.

25. Sanderson and J. C. Scully, "Hydride Formation in Thin Foils of Dilute Ti-Al Alloys," Trans. AIME. Vol. 239, 1883, 1967.

26. E. H. Dix, Jr., R. H. Brown and R. B. Mears, "A Generalized Theory of Stress Corrosion of Alloys," American Society for Testing Materials, 1944.

27. H. W. Pickering and P. R. Swawn, "Electron Metallography of Chemical Attack upon Some Alloys Susceptible to Stress Corrosion Cracking," Corrosion, 19, 373t, 1963.

28. A. M. Yakimova, "Effect of Hydrogen and Oxygen on the Mechanical Properties and Structure of the Titanium Alloy T4," Fiz. Metal. Metalloved., 12, No. 6, 891, 1961.

29. H. Schroeder, "Investigation of the Ordered Phase Ti_3Al Alloys," M. S. Thesis, Ohio State University, 1958.

30. G. Sanderson and J. C. Scully, "Hydride Formation in Thin Foils of Dilute Ti-Al Alloys," Trans. AIME, Vol. 239, 1883, 1967.

31. E. A. Anderson, D. C. Jillson and J. R. Dunbar, "Deformation Mechanisms in Alpha Titanium," Trans. AIME, Vol. 239, 1191, 1953.

32. A. T. Churchman, "The Slip Modes of Titanium and the Effect of Purity on their Occurrence during Tensile Deformation of Single Crystal," Proc. Roy. Soc. A226, 216, 1954.

33. F. C. Rosi, C. A. Dube and B. N. Alexander, "Mechanism of Plastic Flow in Titanium--Determination of Slip and Twinning Elements," Trans. Amer. Inst. Min. Engrs., Vol. 197, 257, 1953.

34. J. C. Williams and M. J. Blackburn, "The Identification of a Non-basal Slip Vector in Titanium and Titanium-Aluminum Alloys," Phys. Stat. Solidi, 25, K1, 1968.

35. R. I. Jaffee, "The Physical Metallurgy of Titanium Alloys," Progress in Metal Physics, Vol. 7, 65, 1958.

36. Harold Margolin and John P. Nielsen, "Titanium Metallurgy," New York University, N. Y. 1958.

37. H. T. Clark, Jr., "The Textures of Cold-Rolled and Annealed Titanium," Trans. Amer. Inst. Min. Engrs. Vol. 188, 1154, 1950.

38. D. N. Williams and D. S. Eppelsheimer, "Cold Rolled Texture of Titanium," Trans. Amer. Inst. Min. Engrs. Vol. 97, 1378, 1953.

39. M. J. Blackburn and J. C. Williams, "Metallurgical Aspects of the Stress Corrosion Cracking of Titanium Alloys," Proceedings of Conference, Fundamental Aspects of Stress Corrosion Cracking, Columbus, Ohio State University, 1969.

40. P. J. Soltis, "Instability and Evidence of Ordering in Ti:8-1-1 Alloy," Trans. AIME, Vol. 233, 903, 1965.

41. F. A. Crossley, "Titanium-Rich End of the Titanium-Aluminum Equilibrium Diagram," Trans. AIME, Vol. 236, 1174, 1966.

42. M. H. Blackburn, "The Ordering Transformation in Titanium -Aluminum Alloys Containing up to 25 at. pct Aluminum," Trans. AIME, Vol. 239, 1200, 1967.

43. J. C. Williams and M. J. Blackburn, "A Comparison of Phase Transformations in Three Commercial Titanium Alloys," Trans. ASM, Vol. 60, 373, 1967.

44. J. M. Peters and J. R. Myers, "Anodic Polarization Behavior of Titanium and Titanium Alloys in Sulfuric Acids," Corrosion, 326, October, 1967.

45. Milton Levy, "Anodic Behavior of Titanium and Commercial Alloys in Sulfuric Acid," Corrosion, 236, August, 1967.

46. Milton Levy and G. N. Sklover, "Anodic Polarization of Titanium and Titanium Alloys in Hydrochloric Acid," J. Electrochem. Soc. Electrochemical Science, 323, March 1969.

47. J. R. Myers, F. H. Beck and M. G. Fontana, "Anodic Polarization Behavior of Nickel-Chromium Alloys in Sulfuric Acid Solution," Corrosion, 1965.

48. M. Codell, "Analytical Chemistry of Titanium Metals and Compounds," Interscience Publishers, N. Y. 1959.

49. J. G. Wilson and A. B. Newall, "General & Inorganic Chemistry," Cambridge University Press, 1966.

50. W. M. Thornton, Jr., "Titanium," American Chemical Society, New York, 1927.

51. D. T. Powell and J. C. Scully, "Stress Corrosion of Alpha Titanium Alloys at Room Temperature," Corrosion, Vol. 24, No. 6, 1968.

52. T. R. Beck, "Stress Corrosion Cracking of Titanium Alloys," J. Electrochem. Soc. Vol. 115, September, 1968.

53. B. F. Brown, "Solution Chemistry within Stress Corrosion Cracks in Ti:8-1-1 Alloy," Presented at Stress Corrosion Cracking Mechanism Conference, Atlanta, Georgia, January, 1971.

54. T. R. Beck, "An Electrochemical Mass Transport-Kinetic Model for Stress Corrosion Cracking of Titanium," J. Electrochem. Soc. February, 1969.

55. M. Pourbaix, "Atlas of Electrochemical Equilibria in Aqueous Solutions," Oxford, N. Y. 1966.

56. N. S. Stoloff and T. L. Johnston, "Crack Propagation in a Liquid Metal Environment," ACTA, Metallurgia. Vol. 11, 251, 1963.

57. J. G. Hines and T. P. Hoar, "The Stress Corrosion Cracking of Austenitic Stainless Steel," J. of Iron and Steel Institute, Vol. 182, 124, 1956.

58. H. H. Uhlig, "New Perspective in the Stress Corrosion Problem," Physical Metallurgy of Stress Corrosion Fracture, Interscience Publishers, 1959.

59. T. P. Hoar and J. M. West, "Mechano-Chemical Anodic Dissolution," Nature, Vol. 181, 835, 1958.